

BIOPHYSICAL AND STRUCTURAL CHARACTERISTICS OF MINK CHANNELS

by

Thanos Tzounopoulos

A DISSERTATION

Presented to the Department of Molecular and Medical Genetics

and the Oregon Health Sciences University

School of Medicine

in partial fulfillment of

the requirements for the degree of

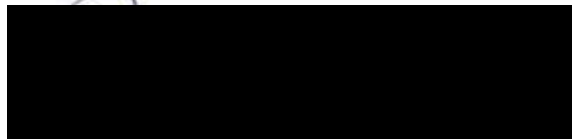
Doctor of Philosophy

November 1996

School of Medicine
Oregon Health Sciences University

CERTIFICATE OF APPROVAL

This is to certify that the Ph.D. thesis of
Thanos Tzounopoulos
has been approved



Professor in charge of the thesis



Member



Member



Member



Member



Associate Dean for Graduate Studies

TABLE OF CONTENTS

Abstract	ix
CHAPTER I: Introduction	1
Ions and ion channels	1
Potassium channels	3
MinK potassium channels	5
Organization of minK gene	6
Membrane topology of the minK protein	6
Biophysical properties of minK currents	6
Pharmacology of minK channels	11
Modulation of minK currents	12
Physiological significance of minK channels	14

Does the minK protein form a K ⁺ channel?	16
Mechanism of minK channel formation	19
Gating mechanism of minK channels	20
CHAPTER II: Materials and methods	21
Molecular biology	21
Site-directed mutagenesis	21
Oocyte expression and electrophysiology	22
Data analysis	22
Computer simulation	23
CHAPTER III: Induction of endogenous channels, in Xenopus oocytes, by high levels of heterologous membrane proteins: MinK is not a chloride channel regulator.	24
Summary	24
Use of Xenopus oocytes as an expression system	24

Expression of membrane and cytoplasmic proteins in <i>Xenopus</i> oocytes	25
Hyperpolarization-activated currents	26
Expression levels and the appearance of hyperpolarization-activated current	33
Conclusions	35
CHAPTER IV: Subunit stoichiometry of minK channels	36
Summary	36
Expression of wild type and mutant minK channels	36
MinK channels are composed of multimers of minK monomers	40
Subunit stoichiometry of minK channels	41
Conclusion	50
CHAPTER V: Gating mechanism of minK channels expressed in <i>Xenopus</i> oocytes	51
Summary	51
Activation and deactivation kinetics	51

Deviation from Cole-Moore prediction	52
Recovery from deactivation	60
Voltage-dependence of reactivation	63
Deactivation kinetics do not reveal more than one,kinetically different, open state	63
Conclusions	70
Chapter VI: Description, discussion and conclusions	71
Is minK a channel , does it require additional subunits, or is it a channel regulator?	71
Structural composition of minK channels	74
How 14 minK subunits form functional K ⁺ channels	76
Gating mechanism	77
Endogenous channel activity in Xenopus oocytes	79
Summary and future directions	81
References	83

LIST OF FIGURES AND TABLES

Figure III-1. Current records from oocytes expressing five membrane and one cytoplasmic protein	27
Figure III-2. Current families in the presence or absence of extracellular Ca^{2+}	29
Figure III-3. Pharmacology of the hyperpolarization-activated current	32
Figure III-4. Relationship between the amount of ShW434F off-gating charge and the hyperpolarization-activated current	34
Table III-1. Ion selectivity in the absence of extracellular Ca^{2+}	31
Figure IV-1. Expression of wild type and mutant minK channels	38
Figure IV-2. Current families induced by injection of wild type and S69A mRNAs	42
Figure IV-3. Analysis of current decrease using a binomial distribution	45
Table IV-1. Kinetic characteristics and voltage dependence of wild type, S69A, and F55A subunits	39

Table IV-2. Kinetics of wild type and coinjection mixtures for voltage commands to -20 mV	47
Figure IV-4. MinK channels formed from 15 subunits	49
Figure V-1. Activation kinetics of minK channels	53
Figure V-2. Deactivation kinetics of minK channels	55
Figure V-3. Effect of holding potential on minK current activation	57
Figure V-4. Time and voltage dependence of the effect of holding potential on minK current activation	58
Figure V-5. Recovery from deactivation	62
Figure V-6. Kinetics of reactivation	64
Figure V-7. Envelope of tails	66
Figure V-1. State model and computer simulations of minK currents	67
Table V-1.	69

Acknowledgments

This is the hardest part of my thesis. It is really hard to isolate the elements of my environment that had a contribution in the accomplishment of this work. It is chaotic and it would lose its beauty if I would try to organize it in a single page, so I will leave it chaotic...

Mother and father thanks for everything in the world, I have a complaint though, why does it have to be so manipulative? I love it, but nevertheless I miss you so much these days...Dad, you are not dead, I still have not forgotten you...

Sir, it has been really fun and frankly all your points have been really well taken...and please never stop making those. Practice your basketball skills, because I will keep on checking on you. I am really glad that at this point the main thought that comes to my brain is "Thank you, my friend...it is always going to be like that".

Jim, thanks for teaching me the fundamentals of electrophysiology. Thanks for being patient and helpful.

Armando, what can I say my friend, things can hardly be described... right or not ?

Bethan, love is a confusing issue isn't it ? but once it is there then you can transform it into plenty of other feelings...it is always going to be there my friend, I have not still got over your pure face and soul (especially, when I compare it to mine...)

and you Vicky, your smile is always going to be with me and so does your melancholic, pretty face. It is OK, isn't it?

Alexa, what are you talking about ? I never understood, are we talking about the same thing ? Is it coincidence, is it the power of emptiness, is it what it was yesterday? but no matter what it is, it is fun, it is educative (yeah right...) it is traveling, dancing, communicating, fighting, making love. Yes, it is being alive. It is there, and your face keeps on getting prettier and prettier.

Anta, I miss you so much, I want to hear your loud laughter, I want to touch your golden hair and talk about our fights, back then when we would whisper to each other until we fell asleep, you remember dont you? "Shhh, you are going to wake up mom and dad and then the mystery is gone"

Abstract

The currents elicited by expression of the minK protein in *Xenopus* oocytes display properties characteristic of K⁺ channels, including voltage-dependent gating, ion selectivity, and blocker pharmacology. However, because of its distinct structure, it is not yet clear whether the minK protein is a K⁺ channel-forming subunit or whether it acts as a regulator of endogenous, otherwise silent channels.

Attali (Attali, 1993) reported that high levels of expression of the minK protein in *Xenopus* oocytes resulted in both a potassium and a chloride current. The K⁺ and Cl⁻ currents were distinguished by their pharmacological and regulatory profiles. These results were interpreted as demonstrating that the minK protein is not a channel-forming protein, but rather an inducer of otherwise silent oocyte channels. However, the hyperpolarization-activated current observed by Attali (Attali, 1993) is pharmacologically indistinguishable from that which is seen following high levels of expression of five structurally and functionally distinct membrane proteins (chapter III). Therefore, the data presented by Attali are based on experimental artifacts and do not address the issue of whether the minK protein forms an ion channel. However, several studies have provided strongly suggestive evidence that the minK protein is a pore-forming subunit (see introduction, chapter I and discussion , chapter VI)

A great deal has been learned about the assembly and structural composition of cloned potassium channels, except for minK. Because of the dramatically different structure of the minK protein, it is unclear how the minK protein might form a potassium channel. To determine whether minK channels are comprised of more than one monomer, and to estimate the subunit stoichiometry of minK channels, the difference in voltage dependence and kinetics between wild type and S69A channels were exploited.

In rat minK, substitution of serine 69 by alanine (S69A) causes a shift in the current-voltage (I-V) relationship to more depolarized potentials; currents are not observed at potentials negative to 0 mV. To determine the subunit stoichiometry of minK channels, wild type and S69A subunits were coexpressed. Injections of a constant amount of wild type mRNA with increasing amounts of S69A mRNA led to potassium currents of decreasing amplitude upon voltage commands to -20 mV. Applying a binomial distribution to the reduction of current amplitudes as a function of the different coinjection mixtures yielded a subunit stoichiometry of at least 14 monomers for each functional minK channel. A model is presented for how minK subunits may form a voltage-dependent, potassium selective pore.

The different structural and functional features of minK suggest a distinct mechanism for voltage-dependent gating. In the experiments described here (chapter V), we used ionic current measurements to examine the different states that minK channels undergo during gating. The main finding is that the kinetic behavior of minK channels deviates from the Cole and Moore prediction and can not be described by an independent gating scheme that involves identical and independent steps. Alternatively, we suggest a simple kinetic model in which minK channels reach a common open state through two different pathways.

CHAPTER I

INTRODUCTION

IONS AND ION CHANNELS

Ion channels are macromolecular pores in cell membranes. When they evolved and what role they may have played in the earliest forms of life is unclear, but today ion channels are most obvious as the most fundamental excitable elements in the membrane of excitable cells.

Physiologists have long known that ions play a central role in the excitability of nerve and muscle. In an important series of experiments from 1881 to 1887, Sidney Ringer showed that the solution perfusing a frog heart must contain salts of sodium, potassium and calcium mixed in a definite proportion if the heart is to continue beating long. Nertst's work (1888) with electrical potentials arising from the diffusion of electrolytes in solution inspired numerous speculations on the ionic origin of bioelectric potentials. Soon, Julius Bernstein (1902,1912) correctly proposed that excitable cells are surrounded by a membrane selectively permeable to K^+ ions at rest and that during excitation the membrane permeability to other ions increases.

During the twentieth century, major cellular roles have been discovered for each of the cations of Ringers solution: Na^+ , K^+ , Ca^{+2} ; as well as for the most of the other inorganic ions of the body fluids: H^+ , Mg^{+2} , Cl^- , HCO_3^- , and PO_4^{-2} .

Excitation and electrical signaling involve the movement of ions through ion channels. The Na^+ , K^+ , Ca^{+2} and Cl^- ions seem to be responsible for almost all the action. Each channel may be regarded as an excitable molecule as it is responsive to some stimulus: a membrane potential change, a neurotransmitter or other chemical stimulus, a mechanical deformation and so on. The channels response, called *gating*, is apparently a simple opening or closing of the pore. The open pore has the important property of selective

permeability, allowing some restricted class of small ions to flow passively down their electrochemical activity gradients at a rate that is very high ($>10^6$ ions per second).

These concepts can be illustrated by using the neurotransmitter-sensitive channels of muscle fibers. At the neuromuscular junction or endplate region of vertebrate skeletal muscle, the nerve axon has the job of instructing the muscle fiber when it is time to contract. Pulse-like electrical messages called *action potentials* are sent down the motor nerve from the central nervous system. When they reach the nerve terminal, action potentials evoke the release of a chemical signal, the neurotransmitter acetylcholine, which in turn diffuses to the nearby muscle surface and causes acetylcholine-sensitive channels to open there. Gating keeps the channel open for a few milliseconds.

How do gated ion fluxes through pores make a useful signal for the excitable tissues? Ion fluxes are electric currents across the membrane and therefore they have an immediate effect on membrane potential. Other voltage dependent channels in the membrane detect the change in the membrane potential, and they in turn become excited. In this way the electric response is made regenerative and self-propagating. This explanation does describe how most signals are propagated, but it is circular. Is the ultimate purpose of excitation to make electricity so that other channels will be excited and make electricity? Clearly not, except in the case of an electric organ. Electricity is the means to carry the signal to the point where a nonelectrical response is generated. As far as is known, this final transduction always starts through a single common pathway: a membrane potential change opens or closes a Ca^{2+} -permeable channel, either on the surface or on an internal membrane, and a Ca^{2+} flux into the cytoplasm is altered, causing a change in the internal free Ca^{+2} concentration. The ultimate response is then triggered by the internal Ca^{+2} ions.

Ion channels are undoubtedly found in the membranes of all cells. Their known functions include establishing a resting membrane potential, shaping electrical signals,

regulating the flow of messenger of Ca ions, controlling cell volume, and regulating the net flow of ions across epithelial cells of secretory and resotptive tissues.

POTASSIUM CHANNELS

The cloning of the different types of ion channels has demonstrated that potassium channels comprise by far the most diverse family. So far five structural patterns have emerged:

(1) *Shaker-like* family of potassium channels. All members of this family share several conserved features: six predicted transmembrane domains (TM), a region contributing to the channel pore between the fifth and sixth TM (P region), and a number of positively charged amino acids in the fourth TM (Kaczmarek, 1991). It is known that four shaker subunits assemble to form a functional channels (MacKinnon, 1991). When expressed in heterologous systems, they give rise to potassium currents that activate upon membrane depolarization. Biophysical aspects such as activation, deactivation and inactivation properties vary among the different members. Within this single superfamily, the channel proteins may be grouped into four subfamilies, based on the original four Drosophila genes, Shaker, Shal, Shab and Shaw (Butler et al., 1989; Salkoff et al., 1992; Tempel et al., 1987). Functional channels may be formed by assembly of 4 subunits, the same or different, within a given subfamily but not between subfamilies.

(2) *inwardly rectifying* potassium channels. Inward rectifiers (IRs) are a distinct, but distantly related to the shaker-like family, potassium channels. They have only two TMs flanking the, conserved among all cloned potassium channels, P region (Ho et al., 1993; Kubo, 1993). Several members of this superfamily have been cloned and so far

six different subfamilies of IRs have been identified. Like the shaker-type channels functional IRs are tetramers which may be homomeric or heteromeric (Yang et al., 1995). Unlike shaker-like subunits, IR subunits from different subfamilies may, in some cases, form heteromeric channels (Tucker et al., 1996). When expressed in heterologous systems, IRs give rise to inward potassium-selective currents upon voltage commands to potentials negative to E_K . IRs do not pass outward current as efficiently as they pass inward current (inward rectification), and this is due to a voltage-dependent block of the pore by intracellular polyamines such as spermine and spermidine (Lopatin et al., 1994), as well as Mg^{2+} (Matsuda et al., 1989). Intracellular binding of cations to the internal part of the pore, inhibits the outward flow of potassium ions at potentials positive to E_K .

(3) TOK1-like channels. The TOK1 subunit structure (Ketchum et al., 1995) appears like a union of a 6 TM subunit of voltage-gated Shaker-like K^+ channel and a 2 TM subunit of inward rectifiers. The functional stoichiometry implied for TOK1 channels is that of a dimer; although this has not been demonstrated. Like voltage-dependent K^+ channels, TOK1 channels produce an outwardly rectifying current when expressed in *Xenopus* oocytes; the channels pass K^+ out of the cell more efficiently than into the cell. TOK1 channels are blocked from passing inward currents in a voltage dependent manner by the presence of divalent cations in the extracellular solution, and they open only at voltages positive to E_K , where the direction of K^+ current flow is outward. In this respect, TOK1 channels have the same gating mechanism as inward rectifiers K^+ channels.

(4) CeK K^+ channels. The CeK channels have a tandem duplication of the IR 2 TM motif. The functional stoichiometry implied for CeK channels is that of a dimer.

Functional features of the CeK channels remain unknown as they have not yet been successfully expressed .

All of the potassium channel-types described above are predicted to have multiple transmembrane domains and a conserved P region. However some ion channel subunits span the membrane only once. Phospholemman is a 15 Kd protein expressed in muscle and liver; it contains only one predicted TM and has limited homology with the γ subunit of the Na^+ , K^+ ATPase (Palmer et al., 1991). When expressed in *Xenopus* oocytes, phospholemman induces a hyperpolarization-activated chloride current (Moorman JR, 1992). Another ion channel with one predicted TM is the influenza virus M2 protein. In *Xenopus* oocytes, the M2 protein induces a monovalent cation channel that is activated by low external pH (Pinto LH, 1992). The M2 protein has no homology to any other known proteins ; it normally exists as disulfide-linked homotetramer (Holsinger and Lamb, 1991). Finally the IsK or minK protein is associated with potassium channel activity and is the main focus of this dissertation.

MinK potassium channels

Heterologous expression of the minK current was first seen by Boyle and coworkers following injection of *Xenopus* oocytes with mRNA isolated from estrogen-primed rat uterus (Boyle et al., 1987). The current activated upon depolarization of the membrane to potentials positive to -40 mV, and did not reach steady state even after prolonged depolarizations. Reversal potential measurements showed that the minK current is carried by potassium ions. Subsequently, the cDNA encoding the minK protein was isolated by expression cloning from a rat kidney cDNA library (Takumi et al., 1988). When expressed in oocytes , minK mRNA induced a current very similar to that induced by uterine mRNA, and the minK protein has since been cloned from rat uterus (Folander et al., 1990; Pragnell et al., 1990).

Organization of the minK gene

The minK protein has no homology with any other known protein. Cloning of the minK from mouse, human and guinea pig has shown a high degree of conservation among the four species. Within the proposed TM domain and flanking regions, the sequence is almost entirely conserved. Southern blots have indicated that minK is a single copy gene in both rat and mouse (Iwai et al., 1990; Lesage et al., 1992). However, Northern blot analyses of rat and mouse mRNA revealed multiple minK transcripts which arise from alternatively spliced 5' untranslated exons and multiple polyadenylation sites (Iwai et al., 1990; Lesage et al., 1992).

Membrane topology of the minK protein

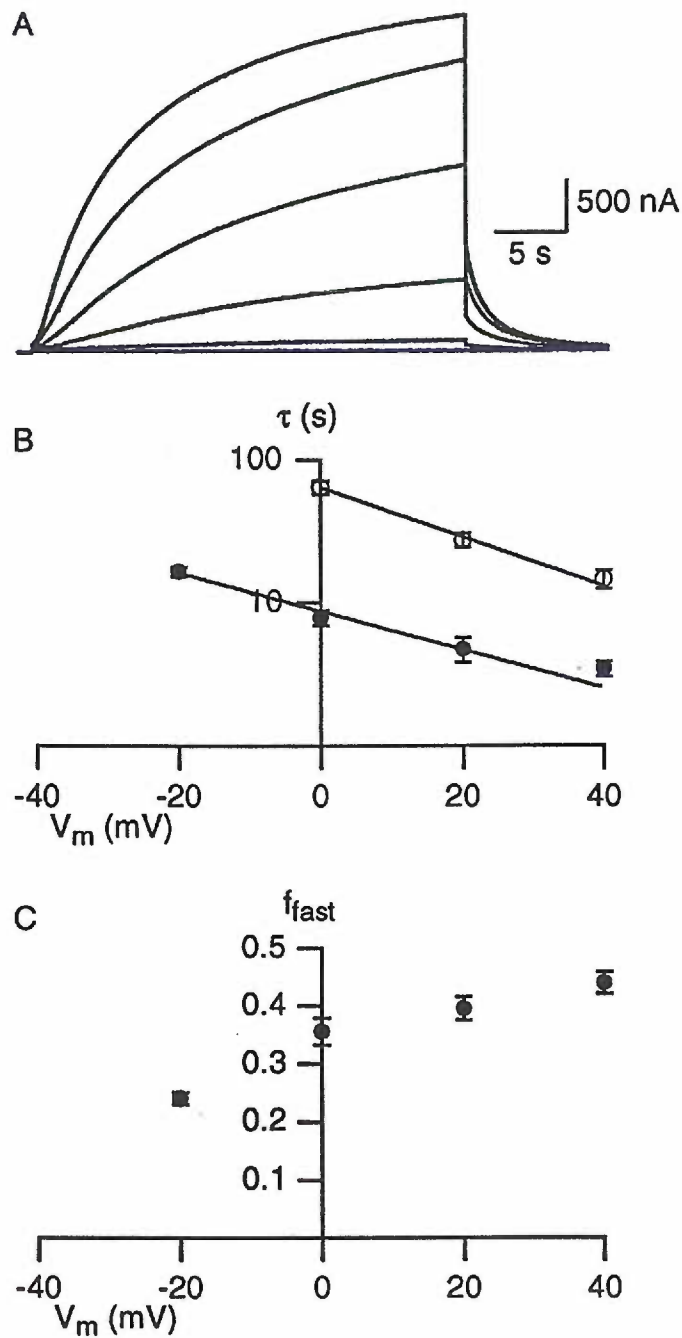
The minK protein is 129-130 amino acids in length and represents a class III bitopic integral membrane protein: a single predicted TM, with the amino-terminus extracellular and the carboxy-terminus intracellular. This topology is supported by previous work (Busch et al., 1992; Varnum et al., 1994), which identified a residue in the C-terminus that is essential for PKC regulation. Additionally, several functional glycosylation sites reside in the amino terminal portion of minK, suggesting its extracellular orientation (Blumenthal et al., 1994)

Biophysical properties of minK currents

Injection of minK mRNA into *Xenopus* oocytes results in slowly activating voltage-dependent, non-inactivating, potassium-selective currents. Figure, V, 1A shows two-electrode voltage clamp recordings of a representative current family evoked by 30s

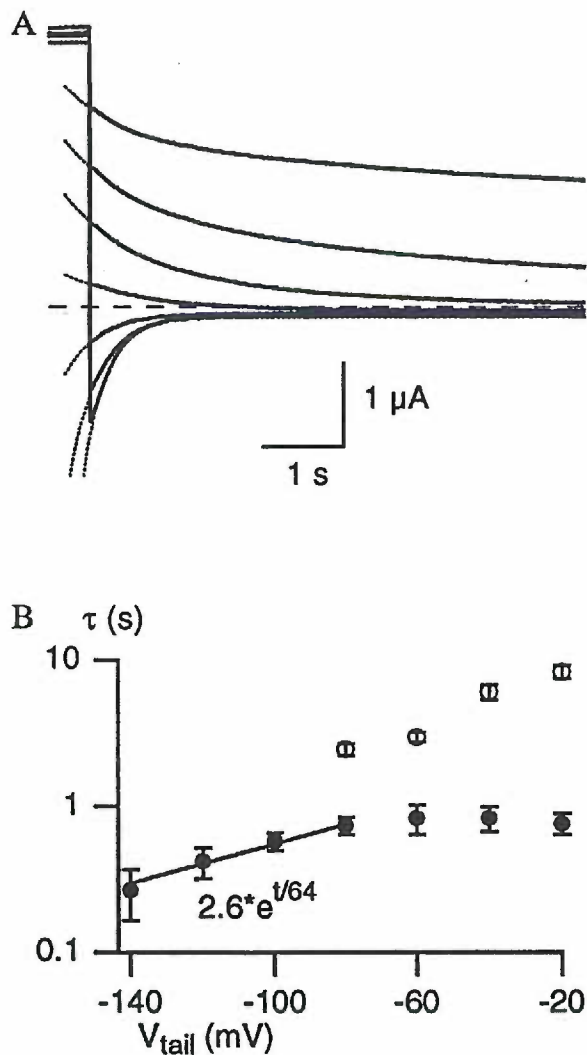
depolarizing commands, from a holding potential of -80 mV to test potentials from -60 to 40 mV. Following depolarization the currents show an initial delay prior to activation and the rising phase was well fit by a double exponential and time constants for the two processes were plotted as a function of the test potential (fig. V, 1B). Both processes are voltage-dependent and the relative contribution of the fast component increases with more depolarized voltages (fig. V, 1C). The tail currents in fig 1A show that the time course of deactivation is faster than activation. Therefore, deactivation kinetics were measured by a protocol in which the membrane potential was stepped to 40 mV for 20 s followed by repolarizing test commands to potentials between -20 and -140 mV. For potentials between -20 and -80 mV the tail currents were well fit by the sum of two exponentials (fig.V, 2A). The two time constants were plotted as a function of the test potential (fig.V, 2B) and demonstrated that deactivation is also voltage-dependent and faster than activation. For potentials more negative than -80 mV, single exponential fits were sufficient to describe the deactivation kinetic properties of the currents. Studies of the open channel current-voltage relationship showed that the current is inwardly rectifying (Blumenthal and Kaczmarec, 1993), the mechanism of this rectification remains unclear. The voltage-dependence of activation determined by applying a Boltzmann function to the instantaneous tail currents as a function of test potential yielded a voltage for half maximal activation equal to -8 mV and the slope factor k was 12.4.

It has not been possible, however, to detect the opening of single minK channels using patch clamp recording. Moreover, preliminary estimates of the single channel conductance from noise analysis have provided conflicting results. For example, noise analysis on patches of membrane from *Xenopus* oocytes suggests that the elementary current step size on depolarizations to 50 mV is about 0.3 fA, which would preclude detection of unitary events with current technology (Yang and Sigworth, 1995). In contrast, non-stationary fluctuation analysis on minK currents from transfected



Figure, V, 1. Activation kinetics of minK channels. Current records from oocytes expressing minK channels (A), time constants of activation plotted as function of the test potential (B), relative amplitude of the fast component plotted against voltage (C). From a holding potential of -80 mV, currents were elicited by 30-s depolarizing commands to potentials

from -60 to 40 mV in 20-mV increments followed by repolarization to a tail potential of -60 mV. Time constants for activation were derived by fitting a sum of two exponentials to the rising phase of the current traces.



Figure, V, 2. Deactivation kinetics of minK channels. Tail currents from oocytes expressing minK channels (A), time constants of deactivation plotted as function of the test potential (B). From a holding potential of -80 mV cells were activated to 40 mV for 20-s and then were repolarized to tail potentials from -20 to -140 mV in 20-mV increments. For potentials between -20 and -80 mV the tail currents were well fit by the sum of two exponentials while for potentials more negative than -80 mV, single exponential fits were used to describe the deactivation kinetic properties of the currents.

embryonic kidney cells has provided an estimate of 1.55 pA for the unitary current recorded at 60 mV (Freeman and Kass, 1994).

Another distinguishing characteristic of minK currents is that their biophysical properties depend on the level of minK protein on the plasma membrane. Using a modified minK gene which contained an epitope tag in the N-terminal domain, Blumenthal, (Blumenthal et al., 1994), showed that the level of protein in the plasma membrane is proportional to the amount of the minK mRNA injected, up to at 50 ng of injected RNA. In contrast, the amplitude of minK currents measured at a fixed time after depolarization, saturates at a lower level of mRNA (1 ng). Injection of higher amounts does not further increase the amplitude of currents, even though the amount of minK protein in the plasma membrane continues to increase.

Although the amplitude of minK currents does not change after a fixed level of minK protein is expressed, the kinetics of the currents can be affected significantly by further increases in the level of expression. In particular, oocytes injected with large amounts of minK RNA have currents that activate more slowly relative to oocytes injected with smaller amounts (Blumenthal and Kaczmarec, 1994; Cui et al., 1994). Because the level of expression increases with time after injection of mRNA into an oocyte, a progressive change in activation kinetics may also be detected in a single oocyte at different times after injection.

Pharmacology of minK currents

The potassium channel blocking ions Ba^{+2} , Cs^{+1} and TEA reduce the amplitude of minK currents. MinK currents can also be blocked by La^{+3} , an effect that is species-specific (Hice et al., 1994). Currents induced by rat or mouse minK channels are sensitive to, 10-50 mM La^{+3} , whereas currents induced by the human minK gene are unaffected by these concentrations.

A number of agents known to block potassium currents in cardiac cells produce a reduction of minK currents expressed in *Xenopus* oocytes. These include clofilium (Honore et al., 1991) and the class III antiarrhythmic agents NE-10064 and NE-10133 (Busch et al., 1994), which also inhibit the slowly activating I_KS current in guinea pig myocytes. In addition, minK currents have also been found to be reduced by the anaesthetic halothane.

Finally, minK currents are affected by fenamates such as niflumic acid, mefenamic acid, flufenamic acid and DIDS. These agents have been traditionally to block chloride currents in *Xenopus* oocytes and other cells. In contrast, these drugs actually produce an increase in minK currents. This is presumed to occur through a stabilization of the open state of the channels, producing a slowing of the rate of deactivation, and at higher concentrations, leading to a persistent activation of minK currents.

Modulation of minK currents

MinK currents in *Xenopus* oocytes may be modulated by a variety of second messengers

such as estrogen, pH, PKC (protein kinase C), cAMP and intracellular calcium.

Estrogens

Heterologous expression of minK currents was first seen in oocytes that had been injected with mRNA from estrogen-primed rat uteri. By preparing uterine RNA from rats at different stages of pregnancy and the estrus cycle, Boyle et al., 1987, showed that the amount of the minK current followed very closely the levels of serum estrogen at the time of preparation, i.e. high at term and proestrus, undetectable at metestrus and midgestation. Following the cloning of minK, it was shown that minK mRNA is not

detectable in the uteri of estrogen-deprived rats, but is expressed at high levels within three hours of estrogen injection (Folander et al., 1990; Pragnell et al., 1990). These results strongly suggest that the minK gene is regulated by estrogens.

pH

MinK currents are modulated by external pH (Yamane et al., 1993). Acidification of the external media results in a decrease in current amplitude with a pK of 5.5 and a Hill coefficient of 1.0. Since this effect is not voltage-dependent, it is most likely due to the protonation of a single acidic residue at a site which is not within the membrane electric field.

PKC

Agents that stimulate PKC, such as phorbol esters and diacylglycerols, inhibit the minK current (Busch et al., 1992; Honore et al., 1992). This effect is blocked by the protein kinase inhibitor staurosporine. The effect of PKC is blocked by mutating serine-103 (S103) on the carboxyl-terminal domain of the protein, indicating that phosphorylation of the minK protein itself causes down regulation (Busch et al., 1992). However, PKC-mediated inhibition of minK currents does not occur in all species. Currents induced by expression of guinea pig minK are enhanced rather than decreased by PKC (Je Zhang et al., 1994; Varnum et al., 1994) and the position analogous to S103 in rat minK is an asparagine in the guinea pig sequence. Conversion of the asparagine to serine results in a PKC-mediated decrease of the current.

cAMP

Changes in the level of intracellular cAMP also produce changes in the amplitude of the minK current, and this is due to the action of the cAMP-dependent kinase (PKA; Blumenthal and Kaczmarek, 1992). Treatments that increased PKA activity led to increases in minK current amplitude, while inhibition of PKA caused the current to decrease. The mechanism through which PKA enhances minK activity is not clear. PKA may directly phosphorylate the channel complex or induce the trafficking of new minK channels to the membrane.

Intracellular calcium

Intracellular calcium ions modulate minK currents. Treatments that raise intracellular calcium levels, such as the ionophore A23187, injection of inositol 1,4,5-triphosphate, or activation of inositol phosphate-coupled receptors (Busch et al., 1992; Honore et al., 1992), produce a voltage-independent increase in the amplitude of minK currents. Conversely, injection of the calcium chelator BAPTA into the oocytes causes a reduction in the current amplitude. Calcium appears to exert its effects through the activation of a protein kinase because similar modulation is achieved by injecting the oocyte with the calcium/calmodulin dependent protein Kinase II (Honore and Lazdunski, 1991) and can be reversed by the calmodulin antagonist W7 (Busch et al., 1992; Honore et al., 1992) or injection of alkaline phosphatase (Honore et al., 1992).

Physiological significance of minK channels

The physiological role should be searched in tissues where minK mRNA has been localized. The first minK localization studies, showed gene expression in glandular epithelial tissues such as kidney, submandibular gland, pancreas, lymphocytes, heart and inner ear (Takumi et al., 1988). The presence of minK protein has been visualized

by immunocytochemistry, which showed dense staining on the apical membranes of epithelial cells in the proximal convoluted and early straight tubule of the kidney, the striated ducts of the submandibular gland, and the stria vascularis of the cochlear duct (Sugimoto et al., 1990). A good candidate for a native current carried by minK channels is found in the epithelial cells of the vestibular labyrinth. In the inner ear, the dark cell epithelium secretes potassium into the lumen of the vestibular epithelium. Cell-attached macro-patch recordings of these cells have revealed a slowly activating potassium-selective current that resembles minK currents (Markus and Shen, 1994). The minK blocking agent clofilium decreases the endocochlear potential when applied into the endolymph (Mori et al., 1993).

The minK protein is also expressed in the uterus but its exact localization is still controversial. Although the original minK currents were induced by RNA extracted from myometrium (Boyle et al., 1987), minK RNA is only detectable in the endometrium by Northern blot. Voltage clamp studies from rat myometrium show a slowly activating potassium current (Mirroneau and Savineau, 1980), but it displays faster activation kinetics and greater sensitivity to extracellular calcium than minK, when expressed in oocytes.

Another candidate for a native current that is carried by minK channels is a slowly activating potassium current that has been recorded in ovarian granulosa cells (Mason et al., 1996). Preliminary characterization of this current indicates that it has all of the electrophysiological and pharmacological features of minK channels.

MinK mRNA is also present in T-lymphocytes (Attali et al., 1992). While no minK-like current has yet been recorded from lymphocytes, clofilium, a minK blocker

prevented induction of interleukin 2 mRNA following mitogen-stimulated T-cell activation.

MinK is highly expressed in rat, mouse, guinea pig and human heart, as shown by Northern blot analysis, PCR, and immunoreactivity. MinK is expressed in both atrium and ventricle (Folander et al., 1990; Freeman and Kass, 1993; Honore et al., 1991; Swanson et al., 1990). The expression of minK in the heart is of particular interest because it is thought to underlie the slow component of the cardiac delayed outward rectifier, I_{Ks} (Varnum et al., 1994). The action potentials of cardiac myocytes are characterized by a prolonged depolarized state and a plateau phase that can last up to a few hundred milliseconds in some cell types. This is in contrast to the action potential of nerve cells that last only a few tens of milliseconds. Repolarization of the action potential results from the activation of one or both of two distinct types of outward K currents, transient outward current (I_{to}) and delayed outward rectifier (I_K). I_K is vitally important for action potential repolarization. Deactivation of I_K may also contribute to the complex balance of currents that determine cardiac pacemaking (Hille, 1992). I_K and its relationship to cardiac function have been extensively studied in guinea pig myocytes (Doerr et al., 1990; Hume and Uehara, 1985; Wettwer et al., 1991) where it has been shown that the class III antiarrhythmic drug E4031, a sotalol derivative, separates I_K into a fast activating, inwardly rectifying current, I_{Kr} , and a slowly activating current, I_{Ks} (Sanguinetti and Jurkiewicz, 1991; Sanguinetti and Jurkiewicz, 1990). MinK and HERG, based on their biophysical, regulatory and pharmacological characteristics are thought to underlie I_{Ks} and I_{Kr} respectively (Varnum et al., 1994); Sanguinetti et al., 1995)

**STRUCTURE-FUNCTION OF minK CHANNELS:
DOES THE minK PROTEIN FORM A K⁺ CHANNEL?**

Although the K^+ current elicited by expression of minK protein in *Xenopus* oocytes displays properties characteristic of K^+ channels, including voltage-dependent gating, ion selectivity, and pharmacology, the structure of the minK protein is unique among cloned K^+ channels. This raised the question as to whether the minK protein represents a voltage-dependent K^+ channel per se or whether it acts as a regulator of endogenous, otherwise silent channels.

Although there is, as yet, no definitive answer to this question, many informative experiments have been performed. Deletion studies indicated that a 63-aminoacid sequence covering the TM domain (containing methionine-1 to valine-9 linked to the region from aspartic acid to lysine-93) is sufficient to elicit K^+ channel activity characteristic of minK. Individual substitutions around the TM domain fell into two classes. Substitutions of residues preceding the TM had no detectable effect, whereas those following the hydrophobic motif drastically reduced channel activity. Thus, the cytoplasmic portion immediately following the TM domain plays a crucial role in the channel activity of minK.

The most compelling evidence that the minK protein forms a potassium channel was the finding that point mutations within the putative TM altered permeation and pharmacological properties (Goldstein and Miller, 1991). Replacement of phenylalanine by threonine at position 55 (F55T) increased the relative permeability of the channel for NH_4^+ and Cs^+ without affecting the ability of the channel pore to exclude Na^+ and Li^+ . Block by two common K^+ channel blockers, TEA and Cs^+ was also modified by the mutation.

Additionally, the mutation from leucine to isoleucine at position 52 (L52I) is very intriguing since channel activity is enhanced in a voltage-dependent manner. Kinetic analysis indicated that the activation process for both wild type and (L52I) is composed of a fast and a slow component. However, for L52I channels the relative contribution

of the fast component was markedly decreased compared to the wild type. This finding, also suggests that the minK protein forms an integral part of the K⁺ channel itself.

In contrast, Attali and coworkers reported that injection of high levels of minK mRNA into *Xenopus* oocytes resulted in the induction of outward K currents at depolarized potentials and inward chloride currents at hyperpolarized potentials, while at low RNA levels only the potassium current was detected (Attali, 1993). Additionally, the K⁺ and Cl⁻ currents were distinguished by their pharmacological and regulatory profiles and mutations were found in the minK protein which selectively abolished either the chloride channel activity or the potassium channel activity. These data were interpreted in a model in which the minK protein acts as a regulator of endogenous, otherwise silent potassium and chloride channels, having a higher affinity for the potassium channel than for the chloride channel. However, this model was disproved by experiments which form part of this dissertation (Tzounopoulos et al., 1995; see Chapter III, below). Consistent with our conclusion, that the minK protein is an integral part of the K channel, Wang (Wang et al., 1996) used scanning cysteine accessibility mutagenesis to identify residues that contribute to the pore; changing residues 44, 45 and 47 to cysteine rendered the channels sensitive to irreversible block by methanethiosulfonateethylsulfonate (MTSES). These data support the hypothesis that minK is a pore-forming subunit, and neither support nor exclude the possibility that minK associates with another subunit to form functional K⁺ channels.

Blumenthal showed that the amplitude of minK currents saturates after injection of only 1 ng of minK mRNA. In addition, successful heterologous expression of minK currents has so far been limited to oocytes and HEK 293 cells, a human embryonic kidney cell line (Freeman and Kass, 1993). Therefore, it has been proposed that minK requires an auxiliary protein for activity. The identity and even the existence of such a protein remains unclear, but possibilities include a cytoskeletal element, a regulatory protein, or

another subunit that contributes structurally to the pore of the channel. Such an auxiliary protein should be present in oocytes and HEK 293 cells but not other cells.

Mechanism of minK channel formation

A great deal is known about the assembly and composition of cloned K channels, except for minK. Because of the dramatically different architecture of the minK protein, it is unclear how the minK protein might form a K⁺ channel. It has been demonstrated that all other cloned potassium channels form by association of four independent subunits, but the number of minK monomers which constitute a functional channel is still unknown. We (chapter V; Tzounopoulos et al., 1995) and others (Wang et al., 1995) have addressed this central question. While the approaches were similar the results were quite different.

These experiments constitute a portion of this dissertation and are presented in detail in chapter IV (see below). To examine this question, we took advantage of some differences in the biophysical characteristics of wild type and a mutant subunit in which an alanine was introduced at position 69 replacing a serine (S69A). In the rat minK protein, this substitution causes a shift in the current voltage relationship to more depolarized potentials; currents are not observed at potentials negative to 0 mV. To determine the subunit stoichiometry of minK channels, wild-type and S69A subunits were coexpressed. When examined at -20 mV, oocytes coinjected with a constant amount of wild type mRNA along with increasing amounts of S69A mRNA led to potassium currents of decreasing amplitude, but with identical biophysical characteristics of the wild type currents. Applying a binomial distribution to the reduction of current amplitudes as a function of the different coinjection mixtures yielded a subunit stoichiometry of at least 14 monomers for each functional minK

channel. A model is presented in chapter IV for how minK subunits may form a channel.

Wang et al by used a similar approach, coexpressing wild type and mutant subunits in which at position 77 a aspartate was replaced by an asparagine, and concluded that 2 minK subunits assemble to form a channel. The discrepancy between the two sets of results is discussed in chapter VI.

GATING MECHANISM OF minK CHANNELS

Based upon our structural model for minK subunit stoichiometry and assembly a gating model was constructed. Since gating current measurements and single channel recordings have not been achieved for minK channels, we relied on ionic current measurements in order to isolate and characterize steps in the activation mechanism of minK channels (Tzounopoulos et al., 1996). We concluded to a simple non-independent state model in which minK channels may reach a common open state via two separate pathways. This is described in chapter V of this dissertation.

CHAPTER II

MATERIALS AND METHODS

Molecular biology

cDNA clones encoding for the rat and guinea pig minK proteins were originally provided by Dr. Michael Varnum, while the human minK cDNA clone was provided by Dr. Bernard Atalli. Routine manipulations were performed as previously described (Adelman et al., 1992, Maniatis) or as is standard. Synthetic mRNA was prepared by in vitro transcription with T7 (from rat minK cDNA) or SP6 (from guinea pig minK cDNA and HERG cDNA) RNA polymerases, in the presence of capping nucleotide G(5')ppp(5')G. To control mRNA concentrations, plasmid DNAs were prepared in parallel and spectrophotometrically quantified. For coinjection experiments appropriate ratios of the DNAs were mixed prior to transcription, and mRNA synthesis was performed using common pools of reagents (see results, chapter IV). Following synthesis, mRNAs were quantified spectrophotometrically and by visual inspection following agarose gel electrophoresis.

Site-directed mutagenesis

Site-directed mutagenesis was performed as previously described (Adelman et al., 1992). Briefly, the minK coding sequence was subcloned into the pSelect phagemid vector and single strand DNA was isolated. The nucleotide sequence was altered by simultaneously annealing a mutagenic oligonucleotide with the required base changes

and an oligonucleotide designed to repair the defective ampicillin resistance gene in the pSelect - vector, followed by complete synthesis of the second DNA strand using T-4 DNA polymerase, and T4 DNA ligase. The reaction products were transformed into a repair deficient strain of E.coli. Plasmid DNA isolated from ampicillin resistant bacteria were retransformed into E.coli strains JM 101 or JM 109. Single stranded M13 and the nucleotide of the mutation was determined using sequenase.

Oocyte expression and electrophysiology

Xenopus laevis care and handling were as previously described (Christie et al., 1990). Briefly , ovaries were surgically removed, oocytes were dissected apart in modified Barths solution, and defolliculated by digestion in calcium-free solution containing collagenase A. Oocytes were injected with RNA using a pressure injector, and incubated at 18 °C with rotary agitation in ND96 (96 mM NaCl, 2 mM KCl, 1 mM MgCl₂, 1.8 mM CaCl, 5 mM HEPES ,pH 7.4). Two to five days after injection macroscopic currents were measured using a two-electrode voltage clamp with a CA-1 amplifier interfaced to an LSI 11/73 computer. Data were filtered at 1kHz and sampled at 50 Hz. During recording, oocytes were continuously superfused with ND-96 at room temperature.

Data analysis

The variability of values from experiments with multiple data points is presented as a mean ± SD with *n* indicating the number of cells contributing to the mean.

The subunit stoichiometry of minK was determined from the binomial theorem applied to the relative current amplitudes for different coinjection mixtures. For a random assembly of subunits the relative current amplitude is given by

$$\sum_{i=0}^n C_i^n \cdot x^{n-i} \cdot (1-x)^i$$

where x = the fraction of wild type subunits, n = subunit stoichiometry, $C_i^n = \frac{n!}{i!(n-i)!}$. For a single subunit sufficient to alter channel function $i = 0$. All data are expressed as mean +/- S.D.

Computer simulation

Kinetic models were generated and evaluated using ScoP, a simulation and model generation environment (Simulation Resources, Barrien Springs, MI). The simulation modeling process was straightforward.

CHAPTER III

Induction of Endogenous Channels by High Levels of Heterologous Membrane Proteins in *Xenopus* Oocytes

Summary

Xenopus oocytes are widely employed for heterologous expression of cloned proteins, particularly electrogenic molecules such as ion channels and transporters. The high levels of expression readily obtained permit detailed investigations without interference from endogenous conductances. Injection of minK mRNA into *Xenopus* oocytes results in expression of voltage-dependent potassium-selective channels. Recent data show that injections of high concentrations of minK mRNA also induce a chloride current with very different biophysical, pharmacological and regulatory properties from the minK potassium current. This led to the suggestion that the minK protein acts as an inducer of endogenous, normally silent oocyte ion channels. We now report that high levels of heterologous expression of many membrane proteins in *Xenopus* oocytes specifically induce this chloride current and a hyperpolarization-activated cation-selective current. The current is blocked by DIDS and TEA, enhanced by clofilium and is pH-sensitive. Criteria are presented which distinguish this endogenous current from those due to heterologous expression of electrogenic proteins in *Xenopus* oocytes. Together with structure-function studies, these results support the hypothesis that the minK protein comprises a potassium-selective channel.

Use of *Xenopus* oocytes as an expression system

Xenopus oocytes have become a widely employed avenue for expression of foreign proteins, most notably electrogenic molecules such as ion channels and transporters. Among the advantages of the oocyte expression system is the ability to obtain high levels of expression, permitting detailed quantitative analysis of currents essentially free of contaminating endogenous currents. Beginning with Shaker, voltage-gated potassium channels have been expressed and extensively studied in Xenopus oocytes, using depolarizing voltage protocols (Christie et al., 1989; Pongs et al., 1988; Timpe et al., 1988). Recently, a new family of potassium channel subunits has been described, the inward rectifiers, and investigation of the structure and function of this family of channels has become a central theme in many laboratories. Inward rectifiers readily pass current at potentials negative to E_K while current is decreased at more positive potentials, therefore hyperpolarizing voltage protocols are employed (Bond, 1994; Dascal et al., 1993; Ho et al., 1993; Kubo, 1993; Kubo et al., 1993). Because of the high levels of expression obtained in Xenopus oocytes, contributions by endogenous channels to current amplitudes are not considered significant. However, under some circumstances this assumption is incorrect and may lead to erroneous interpretations.

Expression of membrane and cytoplasmic proteins in Xenopus oocytes

To further investigate the relationship between expression of the minK protein and ion channel activity in Xenopus oocytes, six structurally and functionally distinct proteins were expressed: the minK protein with a single transmembrane domain (TM) (Blumenthal and Kaczmarek, 1994; Takumi et al., 1988) the six TM, voltage-dependent Shaker potassium channel, ShH4-IR with a mutation, W434F (ShW434F), which eliminates potassium currents but retains gating currents (Taglialatela et al., 1992; Timpe et al., 1988), BIR9, a nonconducting member of the inward rectifier potassium channel family clone predicted to possess two TMs (Bond, 1994), the EAAT2 amino

acid transporter, thought to contain 6-10 TMs (Arriza, 1994), the dopamine D2 G-protein coupled receptor with seven TMs (Bunzow et al., 1988), and the cytoplasmic protein, b-galactosidase. Currents were monitored in the two-electrode voltage clamp. Oocytes injected with minK mRNA showed slowly activating, potassium-selective currents upon prolonged depolarizing commands (Figure III, 1a). Shaker W434F did not demonstrate potassium currents, but short depolarizing commands evoked distinct gating currents (Figure III, 1b; (Tagliatela et al., 1992). Oocytes injected with EAAT2 mRNA resulted in an inward transporter current only upon application of glutamate and at potentials negative to 0 mV (Figure III, 1c; (Arriza, 1994). Oocytes injected with BIR9 mRNA did not produce K⁺ currents different from noninjected oocytes, as previously reported (Figure III, 1d; (Bond, 1994). Dopamine D2 receptors and b-galactosidase are non-conducting molecules and oocytes injected with either of these mRNAs did not show currents different from noninjected oocytes following depolarizing commands (Figure III, 1e, f).

Hyperpolarization-activated currents

When oocytes were examined two days after injection, hyperpolarizing commands evoked little if any time-dependent current. However, when hyperpolarizing commands were delivered four to eight days after injection, oocytes from each group except those expressing b-galactosidase, showed slowly activating, inward currents which were usually not present in noninjected oocytes (Figure III, 1 g-l). Decreasing the external chloride concentration shifted the tail current reversal potential consistent with the Nernst equation for a chloride-selective conductance; the slope of the reversal potential as a function of log [Cl⁻]_o was 53 ± 3 mV/ 10-fold change (n=13, not shown).

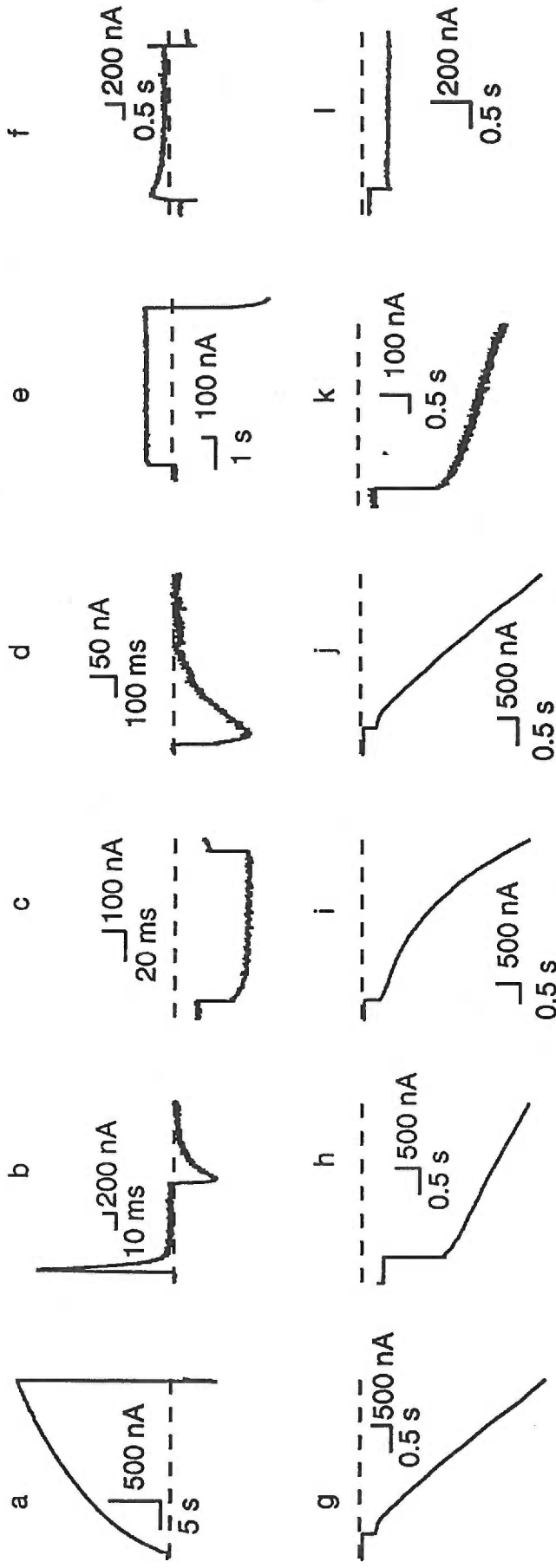


Figure III, 1

Current records from oocytes expressing (a) min K, (b) ShW434F, (c) EAAT-2, (d) BIR9, (e) D2 receptors, (f) b-galactosidase. Min K currents were evoked by 30 second depolarizing commands to 20 mV from a holding potential of -50 mV. ShW434F gating currents were evoked by a 100 ms command to -10 mV from a holding potential of -100 mV; currents were leak corrected. EAAT2 currents were elicited by a 100 ms command to -80 from a holding potential of -30 mV; traces represent the difference of the currents recorded in the presence and absence of 1 mM L-glutamate. Oocytes injected with BIR9 mRNA were recorded in 90 mM K⁺ (substituted for sodium). 500 ms commands to -80 mV were delivered from a holding potential of -10 mV. Oocytes injected with D2 receptor or b-galactosidase mRNA were subjected to 5 s depolarizing commands to 20 mV from a holding potential of -50 mV.

Hyperpolarization-activated inward currents were induced by high levels of expression of membrane proteins, but not b-galactosidase (g-l). Currents were elicited by a 3 s command to -130 mV from a holding potential of -50 mV. For the traces shown, calcium was replaced by cobalt (1 mM). No independent confirmation of the expression or membrane locale of the BIR9 protein was obtained. However, BIR9 is clearly a member of the inward rectifier potassium channel family, and *in vitro* translations of BIR9 mRNA yield a product of the predicted molecular mass (not shown). Efficient expression of dopamine receptors was verified in control experiments by application of dopamine (60 mM), in concert with hyperpolarizing commands, to oocytes coinjected with D2 receptor and GIRK mRNA (Kubo et al., 1993; Dascal et al., 1993); inward potassium currents were detected (not shown). b-galactosidase expression was verified by enzyme assay (Miller, 1972). These sequences, as well as BIR9, were subcloned into pSelect - (Adelman et al., 1992).

The characteristics of this inward current were different among different batches of oocytes. Even within the same batch of oocytes, considerable variability was observed in the amplitude (1-10 μ A) and time course of the appearance of the currents after injection. When calcium was removed from the bath solution, the hyperpolarization-activated current became distinctly more uniform in amplitude and kinetics. Figure III, 2 shows current families and tail currents in the presence (Figure III, 2a, b) and absence (Figure III, 2c, d) of external calcium. With calcium present in the bath solution, large tail currents which reversed direction at approximately -20 mV were observed (Figure III, 2b). However, when calcium was removed from the extracellular solution, tail current amplitudes were greatly reduced and the reversal potentials were no longer shifted by altering the concentration of chloride in the bath solution (Figure III, 2d). Therefore, ion selectivity was investigated in the absence of extracellular calcium. Table III, 1 shows the reversal potentials of the hyperpolarization activated current under biionic conditions for K^+ , Na^+ and Cs^+ . These results demonstrate that in the absence of external calcium, the hyperpolarization activated current is mediated by a nonselective cation channel.

The pharmacology of the hyperpolarization-activated nonselective cation current was investigated in calcium-free bath solution. In all cases, the current was specifically blocked by DIDS (4,4'-diisothiocyanostilbene-2-2'-disulphonic acid), with a 50% inhibitory concentration (IC_{50}) of 0.5 mM ($n=5$, Figure III, 3a), while DIDS had no effect on Shaker W434F gating currents or EAAT2 transporter currents (not shown). In addition, 100 mM TEA blocked approximately 50% of the current (Figure III, 3b). As previously reported, 100 μ M clofilium blocked approximately 50% of the minK potassium current ($n=5$, not shown; 2), while it had no effect on Shaker W434F gating currents or EAAT2 transporter currents (not shown), but in all cases increased the nonselective cation current (Figure III, 3c). Varying the pH of the external solution altered the nonselective cation current; increasing pH from 6.5 to 8.2 decreased the

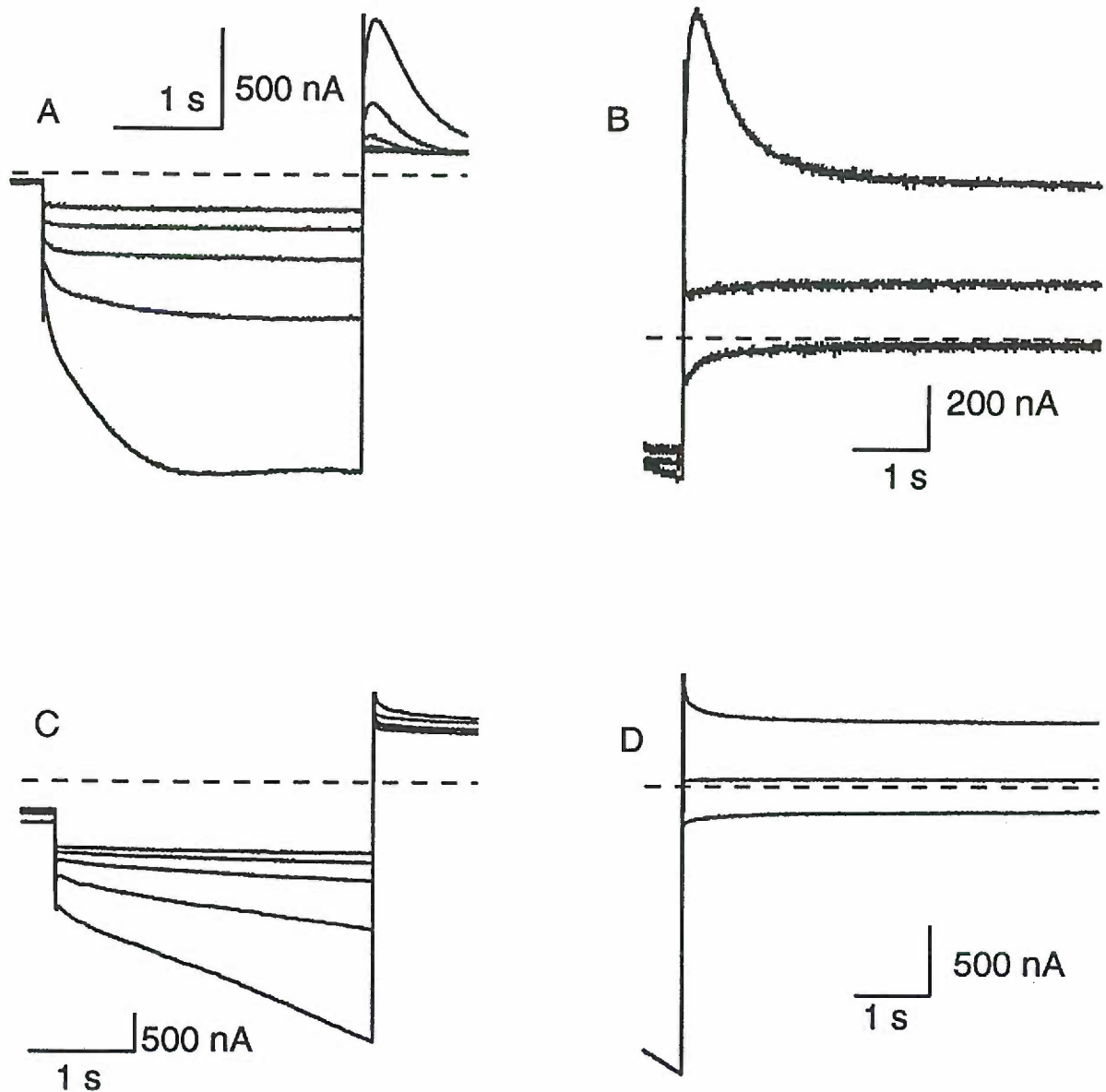


Figure III, 2

Current families and tail currents in the presence or absence of extracellular Ca^{2+} . (a) currents elicited by 3 s commands from -80 to -160 mV in standard recording solution, tail currents measured at 20 mV. (b) tail currents measured in standard recording solution at 20, -20 and -40 mV after a 3 s prepulse to -140 mV. (c) same as in (a) except in the absence of extracellular Ca^{2+} . (d) tail currents measured at 20, -40, and -60 mV after a 3 s

prepulse to -140 mV. Bath solution contained 180 mM mannitol, 10 mM HEPES, 1 mM MgCl₂ and 10 mM KCl (predicted ECl⁻ ≈ -19 mV).

Table 1: Ion selectivity in the absence of extracellular Ca^{+2}

	K^+	Na^+	Cs^+
E_{rev} (mV)	-50 ± 3	-52 ± 2	-53 ± 2
P_X/P_K	1 ± 0.1	0.92 ± 0.1	0.88 ± 0.1

Reversal potentials were measured under biionic conditions, with 10mM of the indicated cation in the external solution which also contained 180mM mannitol, 10mM Hepes and 1mM MgCl_2 . Values represent the mean \pm SEM of 4-6 oocytes. Permeability ratios are defined as $P_X/P_K = \exp(F\Delta E_{\text{rev}(x-k)}/RT)$, where $\Delta E_{\text{rev}(x-k)} = E_{\text{rev},X} - E_{\text{rev},K}$.

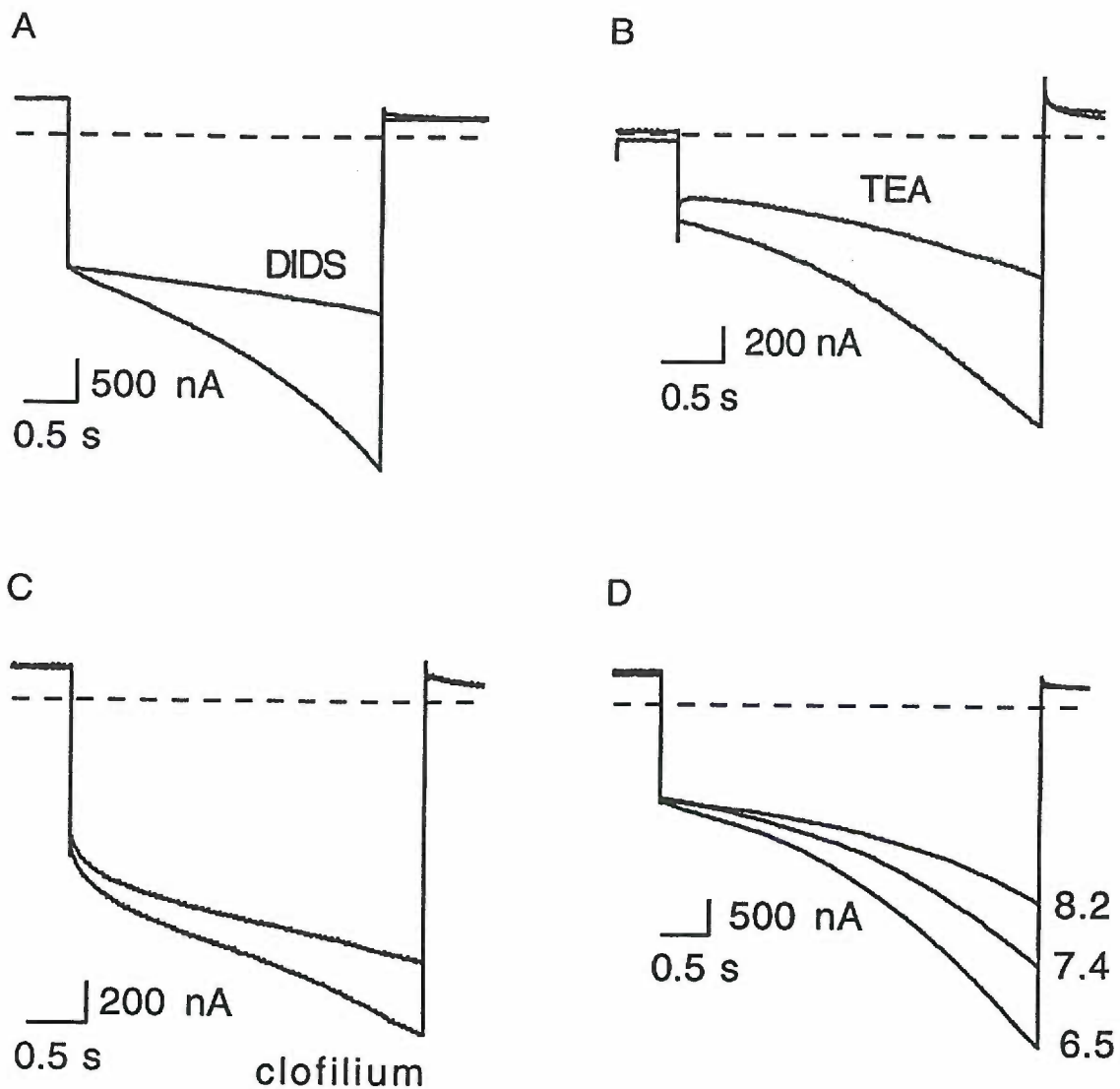


Figure III, 3
 Pharmacology of the hyperpolarization-activated current. Effect of: (a) DIDS (1 mM), (b) TEA (100 μ M), (c) clofilium (100 μ M), (d) alteration of external pH. Oocytes injected with EAAT2 mRNA were recorded 4-7 days after injection in the absence of externally applied L-glutamate. Following a 3 s prepulse to 20 mV, currents were elicited by 3 s hyperpolarizing commands to -130 mV from a holding potential of -50 mV. To block residual calcium channels and screen surface charge, calcium was replaced by cobalt (1 mM) in the standard recording solution.

current by approximately 40% (n=12, Figure 3d). Similar results were obtained in calcium-containing bath solution, demonstrating that this current is the same as that previously reported for oocytes expressing high levels of the minK protein (Attali, 1993).

Expression levels and appearance of the nonselective cation current

The hyperpolarization-activated nonselective cation current was not usually detected until high levels of heterologous expression were achieved. Oocytes injected with the same amount of ShW434F mRNA were studied at progressively later times after injection. Figure III, 4 shows the relationship between the amount of ShW434F off-gating charge, which presumably correlates with the number of channels in the membrane, and the appearance of the hyperpolarization-activated nonselective cation current. Although gating currents were clearly present, the nonselective cation current was not detected until gating charge movement surpassed 8 nC in magnitude. Similar results were obtained for each of the membrane proteins; only at relatively late times after injection was the hyperpolarization-activated nonselective cation current detected.

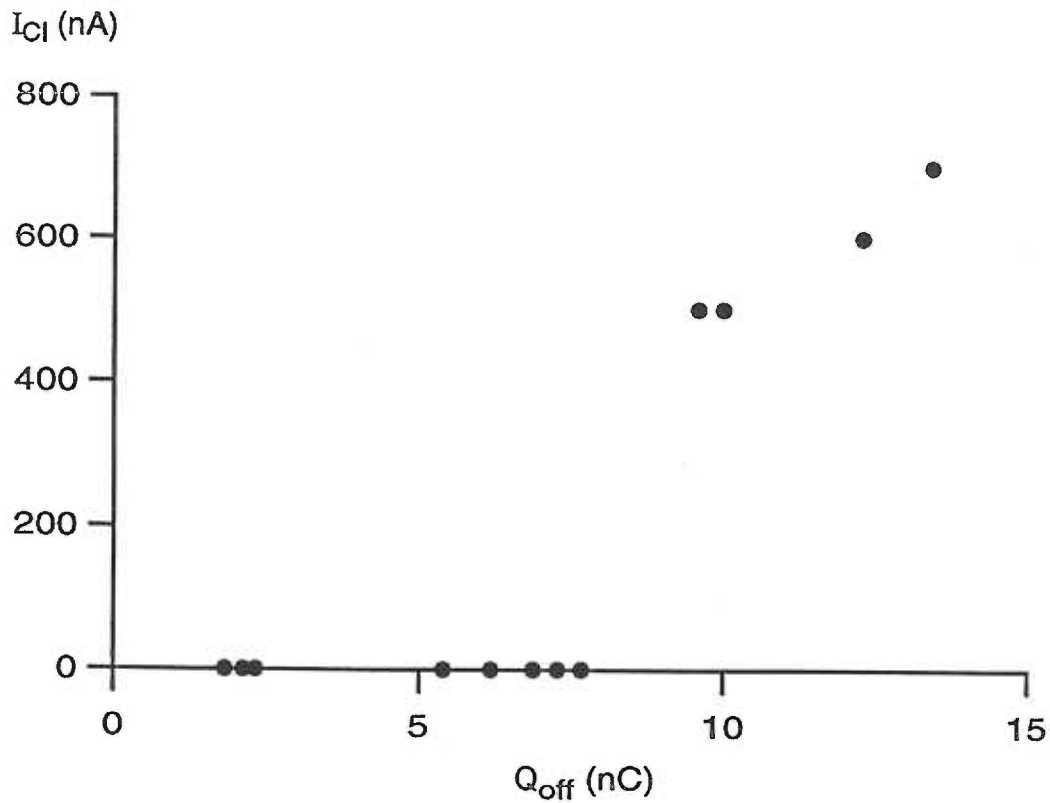


Figure III, 4

Relationship between the amount of ShW434F off-gating charge and the hyperpolarization-activated chloride current. Oocytes were injected with the same amount of mRNA and studied at progressively later times after injection. Currents were evoked as described in Figure 1. The off-gating charge (Q_{off}) was obtained as the integral of the off-gating current. Total capacitance ranged from 200-225 nF. Each data point represents a single oocyte.

Conclusions

High levels of expression of membrane proteins in *Xenopus* oocytes results in the induction of an endogenous, hyperpolarization-activated currents. In the presence of calcium, the current is composed of two components, a calcium activated chloride current and a non selective cation current. When calcium is eliminated from the extracellular solution, only the non selective cation current remains. The hyperpolarization-activated current is blocked by DIDS and TEA, accentuated by clofilium and is pH-sensitive.

These data refute the model proposed by Attali et al, that min K is a regulator of endogenous silent potassium or chloride channels because the chloride current they recorded was an artifact of heterologous overexpression in oocyte.

CHAPTER IV

MinK Channels Form by Assembly of at Least 14 Subunits

Summary

Injection of minK mRNA into *Xenopus* oocytes results in expression of slowly activating, voltage dependent potassium channels, distinct from those induced by expression of other cloned potassium channels. The minK protein also differs in structure, containing only a single predicted transmembrane domain. While it has been demonstrated that all other cloned potassium channels form by association of four independent subunits, the number of minK monomers which comprise a functional channel is unknown. In rat minK, substitution of serine 69 by alanine (S69A) causes a shift in the current-voltage (I-V) relationship to more depolarized potentials; currents are not observed at potentials negative to 0 mV. To determine the subunit stoichiometry of minK channels, wild type and S69A subunits were coexpressed. Injections of a constant amount of wild type mRNA with increasing amounts of S69A mRNA led to potassium currents of decreasing amplitude upon voltage commands to -20 mV. Applying a binomial distribution to the reduction of current amplitudes as a function of the different coinjection mixtures yielded a subunit stoichiometry of at least 14 monomers for each functional minK channel. A model is presented for how minK subunits may form a voltage-dependent, potassium selective pore.

Expression of wild type and mutant minK channels.

Depolarizing voltage commands delivered to *Xenopus* oocytes injected with wild type minK mRNA evoked slowly activating, voltage-dependent potassium currents not present in uninjected oocytes. Channel kinetics and voltage dependence of activation were examined. Fitting the rising phase of the current traces at 20 mV with the sum of two exponentials (Fig IV, 1a), yielded activation time constants of $t_{fast} = 3.5 \pm 0.5$ s and $t_{slow} = 26 \pm 1.3$ s with relative amplitudes of 0.27 and 0.73, respectively ($n = 5$). Following repolarization to -60 mV the channels deactivated with a time course which was best fitted by the sum of two exponential functions, yielding time constants of $t_{fast} = 0.55 \pm 0.1$ s and $t_{slow} = 3.0 \pm 0.4$ s, with relative amplitudes of 0.5 for each component ($n = 5$). Voltage dependence of activation was determined by applying a Boltzmann function to the instantaneous tail currents as a function of test potential between -60 and 40 mV; a double-exponential was fitted to tail currents and extrapolated to the beginning of the tail pulse. The voltage for half-maximal activation, $V_{1/2}$, was -8 ± 2 mV and the slope factor, k , was 12.4 ± 0.3 mV ($n = 5$; Table IV, 1).

Serine 69 is predicted to reside at the cytoplasmic border of the transmembrane domain. Introduction of S69A in rat minK resulted in altered voltage-dependence and kinetics at potentials between -60 and 40 mV (Fig IV, 1b). Activation kinetics of S69A channels examined by fitting a sum of two exponentials to the rising phase of the current trace at 20 mV (Fig IV, 1b) yielded time constants that were decreased compared to wild type channels, $t_{fast} = 2.1 \pm 0.1$ s and $t_{slow} = 20.3 \pm 1$ s, and relative amplitudes of 0.36 and 0.64, respectively ($n = 5$). Deactivation kinetics were also significantly faster than wild type channels; $t_{fast} = 0.24 \pm 0.05$ s and a $t_{slow} = 1.9 \pm 0.1$ s, and relative amplitudes of 0.88 and 0.12, respectively ($n = 5$). The Boltzmann parameters of S69A channels revealed a shift to more positive potentials, $V_{1/2} = 15 \pm 2$ mV and $k = 9.4 \pm 0.3$ mV ($n = 5$; Table IV, 1). Indeed, currents from oocytes expressing S69A are only detected at potentials positive to 0 mV; no currents could be detected at -20 mV. This made

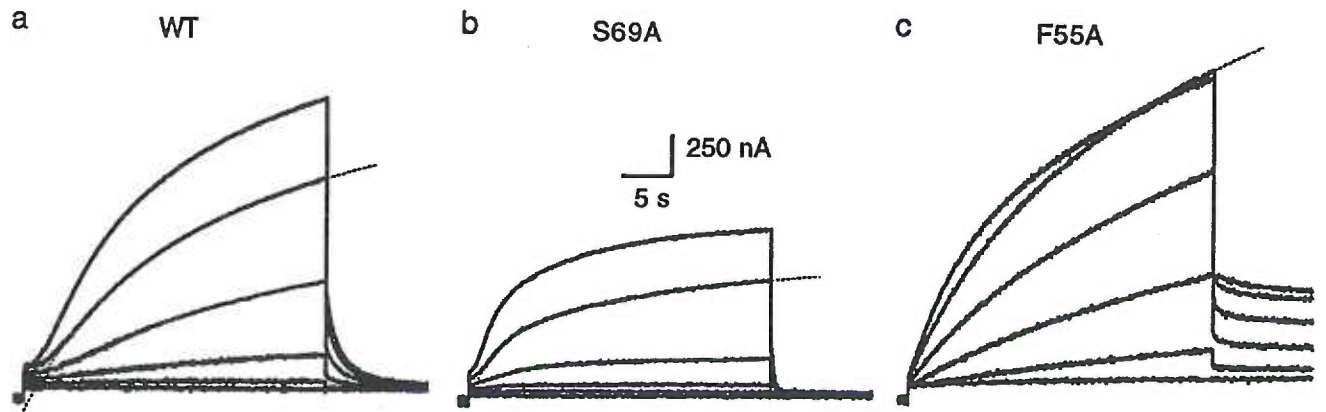


Figure IV,1. Expression of wild type and mutant min K channels.

Current records from oocytes expressing (a) Wild type min K channels, (b), S69A min K channels, and (c) F55A min K channels. From a holding potential of -80 mV, currents were elicited by 30s depolarizing commands to potentials from -60 to 40 mV in 20 mV increments. The traces at 20 mV are presented with fits of a double-exponential function. For the traces presented in (c), a 10 s prepulse to -120 mV was applied prior to depolarization. The initial jump apparent in some records is due to an endogenous chloride current. For wild type and F55A, 5 ng of mRNA was injected; 50 ng of S9A mRNA was injected.

Table 1: Kinetic characteristics and voltage dependence of wild type, S69A and F55A channels.

	WT _{act}	WT _{deact}	S69A _{act}	S69A _{deact}	F55A _{act}	F55A _{deact}
τ_f (s)	3.5±0.5	0.5±0.1	2.1±0.1	0.2±0.05	5.6±0.5	2.5±0.2
τ_s (s)	26.0±1.3	3.0±0.4	20.3±1.0	1.9±0.1	38.5±1.3	4.4±0.4
A _f	0.27	0.50	0.36	0.88	0.15	0.50
V _{1/2} (mV)	-8±2		15±2		-26±2	
k (mV)	12.4±0.3		9.4±0.3		13.4±0.3	

Activation kinetics were examined by fitting a sum of two exponentials to the rising phase of the current trace at 20 mV. Following repolarization to -60 mV channel deactivation time course was fit by a sum of two exponentials. Voltage dependence of activation was determined by applying a Boltzmann function, $1/1+e^{-(V-V_{1/2})/k}$, to the instantaneous tail current as a function of test potential between -60 and 40 mV. A_f is the relative contribution of the fast component. n = 5 for all measurements; errors are S.D.

analysis of S69A currents difficult due to contamination by endogenous sodium channels which are activated at potentials positive to 20 mV.

Another point mutation was also examined. Phenylalanine at position 55 was substituted by alanine (F55A); this residue is predicted to reside within the transmembrane domain. Expression of this mutant resulted in current amplitudes not different from wild type (Fig IV, 1c). However, activation kinetics were altered, with $t_{fast} = 5.6 \pm 0.5$ s and $t_{slow} = 38.5 \pm 1.3$ s, and relative amplitudes of 0.15 and 0.85, respectively ($n = 5$). Deactivation kinetics at -60 mV yielded time constants that were larger than wild type, $t_{fast} = 2.5 \pm 0.2$ s and $t_{slow} = 4.4 \pm 0.4$ s, with relative amplitudes of 0.49 and 0.51, respectively ($n = 5$). The voltage dependence of F55A channels was shifted to more negative potentials compared to wild type; $V_{1/2} = -26 \pm 2$ mV and $k = 13.4 \pm 0.3$ mV ($n = 5$) (Table IV, 1). Thus, compared to wild type channels the substitution F55A shifted voltage-dependence to more negative potentials, and tail currents for all test potentials deactivated significantly slower than wild type.

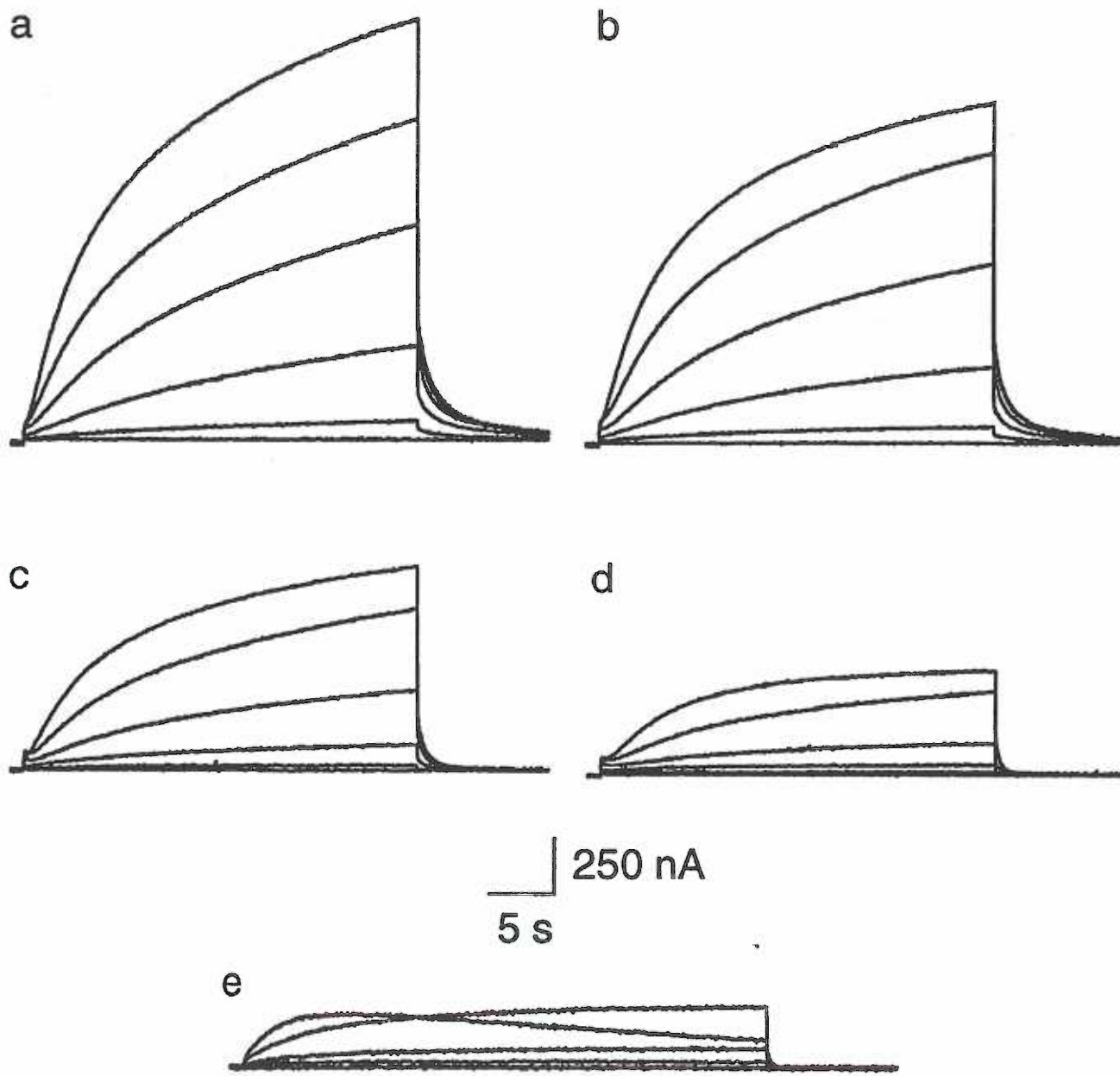
MinK channels are composed of multimers of minK monomers

To test whether minK channels are composed of multimers of minK monomers, wild type and mutant subunits were coexpressed. Plasmids, differing only in a single nucleotide, which contain either wild type or mutant minK coding sequences, were prepared in parallel. DNAs were qualitatively compared by agarose gel analysis and quantified by spectrophotometry. Equal amounts of DNA were linearized and mRNAs were synthesized using common pools of reagents; in vitro synthesized mRNAs were also qualitatively and quantitatively evaluated (see methods). In addition, it has been previously shown that S69A and wild type mRNAs produce equal amounts of membrane-bound minK subunits (21). Figure IV, 2 shows current families after

coinjection of a constant amount of wild type mRNA together with water (a), or varying amounts of S69A mRNA (b-d). Coinjected oocytes displayed reduced current amplitudes compared to wild type at all potentials tested. The current amplitude reduction demonstrates that S69A subunits have a dominant negative effect on coexpressed wild type subunits, suggesting that wild type and S69A subunits coassemble. Complementary results were obtained when a constant amount of F55A was coinjected with varying amounts of wild type (not shown). In this case, the voltage dependence of the mutant is shifted to more negative potentials, resulting in decreased current amplitudes at potentials below -40 mV due to dominant negative effects of wild type subunits, while at more positive potentials the current amplitudes are increased due to the additional contribution of channels comprised of either wild type subunits or wild type and F55A subunits. Therefore, minK channels are comprised of more than one subunit.

Subunit stoichiometry of functional minK channels.

As discussed above, coinjection of increasing amounts of S69A mRNA with a constant amount of wild type mRNA resulted in current amplitudes that were smaller than wild type alone. To assess the subunit stoichiometry of minK channels in oocytes injected with different ratios of wild type and S69A mRNAs, a binomial distribution was applied to tail current amplitudes at -60 mV following a test pulse to -20 mV. The analysis presented below assumes that: 1) wild type and mutant channels express equally, 2) the different subunits assemble randomly, and 3) one S69A subunit abolishes channel function at -20 mV. At this voltage, channel kinetics from all coinjection mixtures were indistinguishable from wild type, suggesting that only wild type channels contribute to the current at -20 mV. In contrast, channel kinetics following test pulses to 20 mV showed increasing rates of deactivation at -60 mV as the



Figure, IV, 2. Current families induced by injection of wild type and S69A mRNAs.

(a) Current records from an oocyte injected with wild type only mRNA (5 ng); (b-d) Currents

recorded following coinjection of a constant amount of wild type (5 ng) with relative amounts of S69A mRNA (0.01, 0.1, or 1); (e) Current records from an oocyte injected with only S69A mRNA (5 ng). Exponential fits for traces recorded at 20 mV are superimposed; voltage protocols are the same as in figure 1a, b.

amount of S69A mRNA was increased, suggesting that channels comprised of both wild type and S69A subunits contribute to the current at 20 mV. Current traces evoked by test pulses to -20 mV and 20 mV from oocytes injected with a constant amount of wild type plus various amounts of S69A mRNAs are presented in Figure IV, 3a and 3c, respectively. The difference in kinetics is apparent from the tail currents; these are presented, with double-exponential fits, in Figure IV, 3b (following test pulses to -20 mV) and 3d (following test pulses to 20 mV). To determine the minimum number of minK subunits which assemble to form the channel, tail current amplitudes following test pulses to -20 mV from the various mixtures were plotted as a function of the ratio of wild type to S69A mRNA. The data points were fitted to the first term of the binomial expression, according to the formula $f = ([\text{wild type}]/([\text{wild type}] + [\text{S69A}]))^n$, where f = the ratio of the current amplitudes from mixture injections to wild type alone. $[\text{wild type}]$ is the constant concentration of wild type mRNA, $[\text{S69A}]$ is the concentration of S69A mRNA, and the exponent, n , is the number of subunits per functional channel. Using this formula, the data were best fit when $n = 13.7$, suggesting that at least 14 minK monomers assemble to form functional channels (Figure IV, 3e). For comparison, curves for $n = 10$ and $n = 18$ are also shown.

Analogous experiments were performed using oocytes coinjected with a constant amount of F55A and varying amounts of wild type mRNAs. As the amount of wild type mRNA was increased, the tail current amplitudes at -60 mV following a test pulse to -40 mV were reduced compared to oocytes injected with F55A mRNA alone, and retained the kinetic characteristics of F55A. Analysis of the current amplitude reduction as a function of the different coinjection mixtures yielded an estimate of at least 14 subunits per functional channel, in agreement with the results independently obtained from coinjections of wild type and S69A mRNAs.

How might such a molecule form an ion channel? When channels are formed by identical subunits, it is generally assumed that the subunits have the same conformation

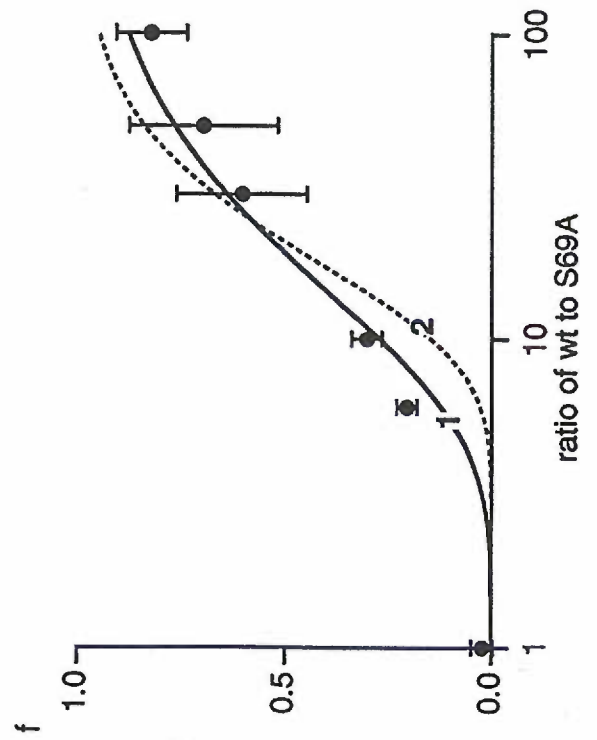
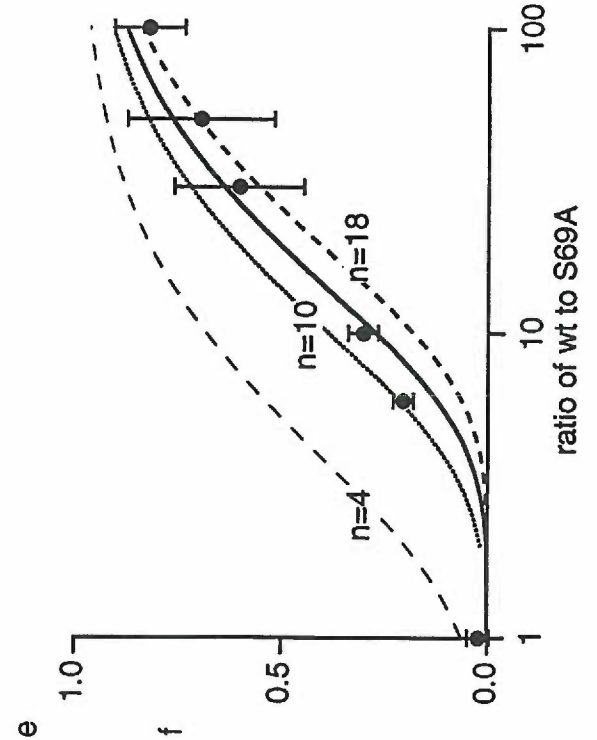
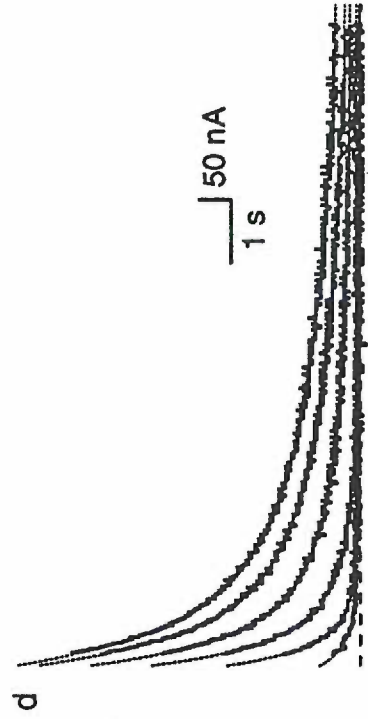
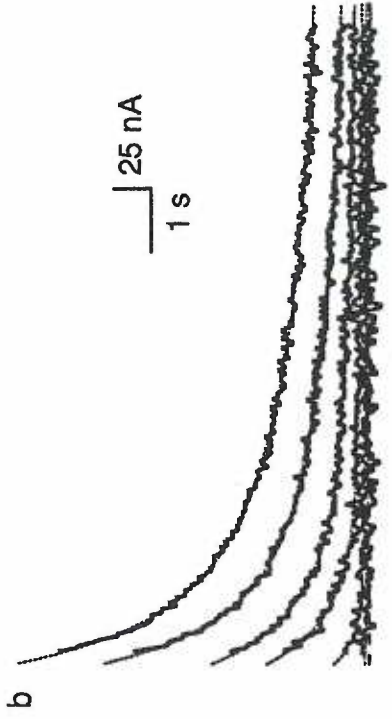
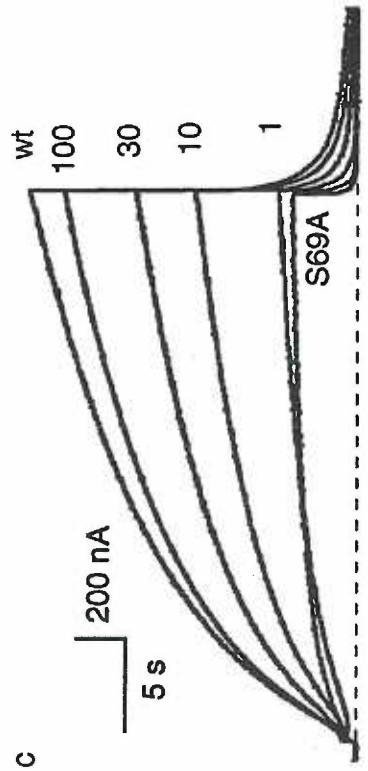
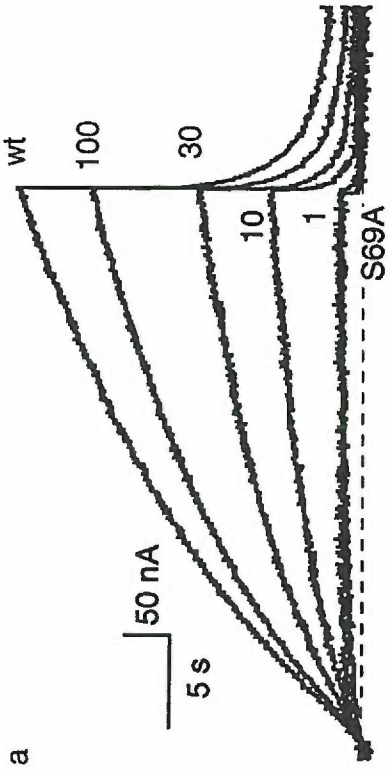


Figure 3. Analysis of current decrease using a binomial distribution.

Superimposed current records at -20 mV (a) and 20 mV (c) recorded from oocytes injected with different ratios of wild type to S69A mRNAs. The six traces represent wild type mRNA alone, coinjection of wild type + S69A mRNAs in proportions denoted as the ratio of wild type to S69A (100, 30, 10, 1), and S69A mRNA alone. Tail currents (b, d) were measured after a 30s depolarizing step to -20 mV (b) or 20 mV (d) and repolarization to -60 mV. Tail current traces are presented with double-exponential fits; note the change in kinetics apparent following test pulses to 20 mV. For all coinjections, the amount of wild type mRNA was kept constant (5 ng) and the amount of S69A was varied.

To determine the minimum number of subunits which form min K channels, the binomial distribution was applied (e). Following depolarizations to -20 mV, the instantaneous tail currents at -60 mV were determined by fitting the traces with a sum of two exponentials and extrapolating back to the beginning of the tail pulse. These values were normalized to the tail current amplitude for oocytes injected with wild type mRNA alone, and plotted as a function of the ratio of wild type to S69A mRNA. Shown is a fit of the first term of the binomial expression $f = \frac{[\text{wild type}]}{([\text{wild type}] + [\text{S69A}])^n}$ where f = current amplitude of the coinjection mixture/current amplitude of wild type alone, $[\text{wild type}]$ is the concentration of wild type mRNA, $[\text{S69A}]$ is the concentration of S69A mRNA, and n is the subunit stoichiometry. The data was best fit with a value of $n = 13.7$ (solid line). Also shown are relations for $n = 4, 10$ and 18 as indicated.

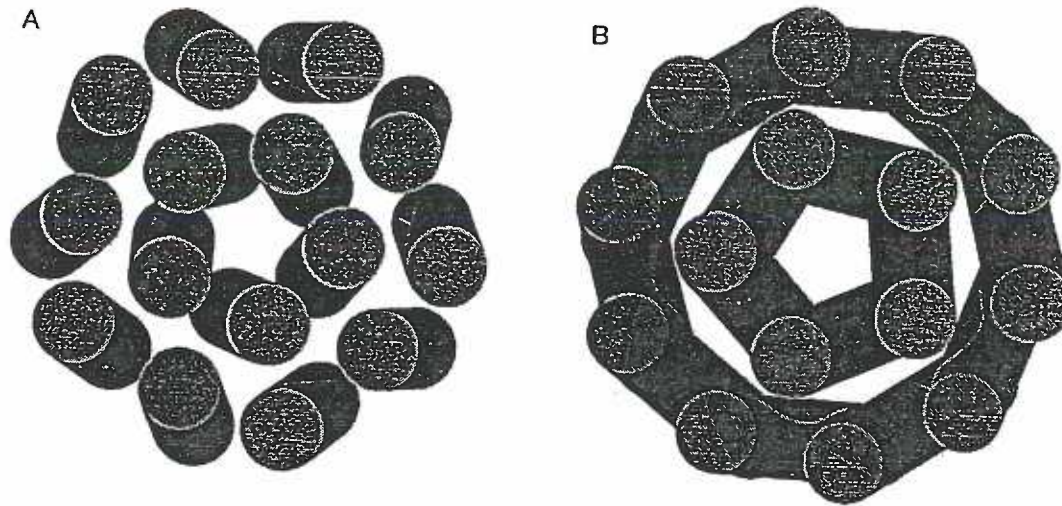
Table 2: Kinetics of wild type and coinjection mixtures for voltage commands to -20 mV.

	WT _{act}	WT _{deact}	1WT+	1WT+	1WT+	1WT+	1WT+
			0.01S69A _{act}	0.01S69A _{deact}	0.1S69A _{act}	0.1S69A _{deact}	0.1S69A _{deact}
τ_f (s)	10 \pm 1	0.5 \pm 0.2	10.7 \pm 1.0	0.5 \pm 0.1	10.5 \pm 0.5	0.5 \pm 0.1	0.5 \pm 0.1
τ_s (s)	ND	3.1 \pm 0.1	ND	2.8 \pm 0.2	ND	3.0 \pm 0.1	3.0 \pm 0.1
A_f	0.14	0.50	0.12	0.50	0.13	0.55	0.55

Activation kinetics were examined by fitting a sum of two exponentials to the rising phase of the current trace at -20 mV. Following repolarization to -60 mV channel deactivation time course was fit by a sum of two exponentials. A_f is the relative contribution of the fast component. $n = 4$ for all measurements; errors are S.D.

and are related by radial symmetry about the axis of the pore. If minK channels are formed by assembly of at least 14 identical subunits, they cannot be arranged with 14-fold radial symmetry because the pore would be very large. We postulate that minK channels assemble in two stages. First, three monomers associate into a trimeric structure with three-fold symmetry in which the TM helices form triple stranded coiled-coils.

The channel is hypothesized to form by the assembly of multiple trimers. Although the data are best fit if at least 14 subunits assemble to form minK channels, the packing of the helices is greatly improved if the channel is formed by five trimers, a "pentamer-of-trimers" with five-fold radial symmetry, in which the pore is formed from five internal subunits surrounded by ten outer subunits (Figure IV, 4a). More details about the structural model are given in the discussion of this dissertation (chapter VI).



Figure, V, 4. Min K channels formed from 15 subunits.

A) Five trimers of min K subunits associate into a "pentamer of trimers". Each trimer has a three-fold degree of symmetry and the channel has a five-fold degree of symmetry. In this closed state, positively charged residues block access to the pore.

B) Following depolarization, the channel undergoes a rearrangement such that the central five helices shift from a left handed to a right handed spiral around the axis of the pore. The positively charged residues are removed from the vicinity of the pore and the channel is capable of ion conduction.

Conclusions

Based on the assumptions discussed earlier on this chapter, we concluded that fourteen monomers of the minK protein assemble to form functional channels. If minK channels are formed by assembly of 14 identical subunits, they cannot be arranged with 14-fold radial symmetry because the pore would be very large. We postulate that minK channels assemble in two stages. First, three monomers associate into a trimeric structure with three-fold symmetry in which the TM helices form triple stranded coiled-coils. Each trimer has classic "knobs-into-holes" helix packing, typical of coiled-coils, and each of the subunits occupies an equivalent position. Then five trimers are coming together to form the functional channel in which the pore is formed from five internal subunits surrounded by ten outer subunits. This is a speculative model based only on the number of minK monomers that come together to form functional channels, but is consistent with the stoichiometry and the need to accommodate pore size and selectivity.

Finally, our data do not exclude the possibility of additional(s) auxiliary non-minK subunits in the functional channel-complex.

CHAPTER V

Gating of minK channels expressed in *Xenopus* oocytes.

Summary

The probability of opening for voltage-dependent ion channels is determined by changes in the transmembrane potential. The activation process requires a series of conformational transitions in the channel protein, particularly the movement of charged residues within the membrane electric field, which is manifested as gating currents (Armstrong and Bezanilla, 1973). For many voltage-gated channels, measurements of gating and ionic currents have provided insight into the different closed and open conformational states (Bezanilla et al., 1994; Stefani et al., 1994; Zagotta, 1994).

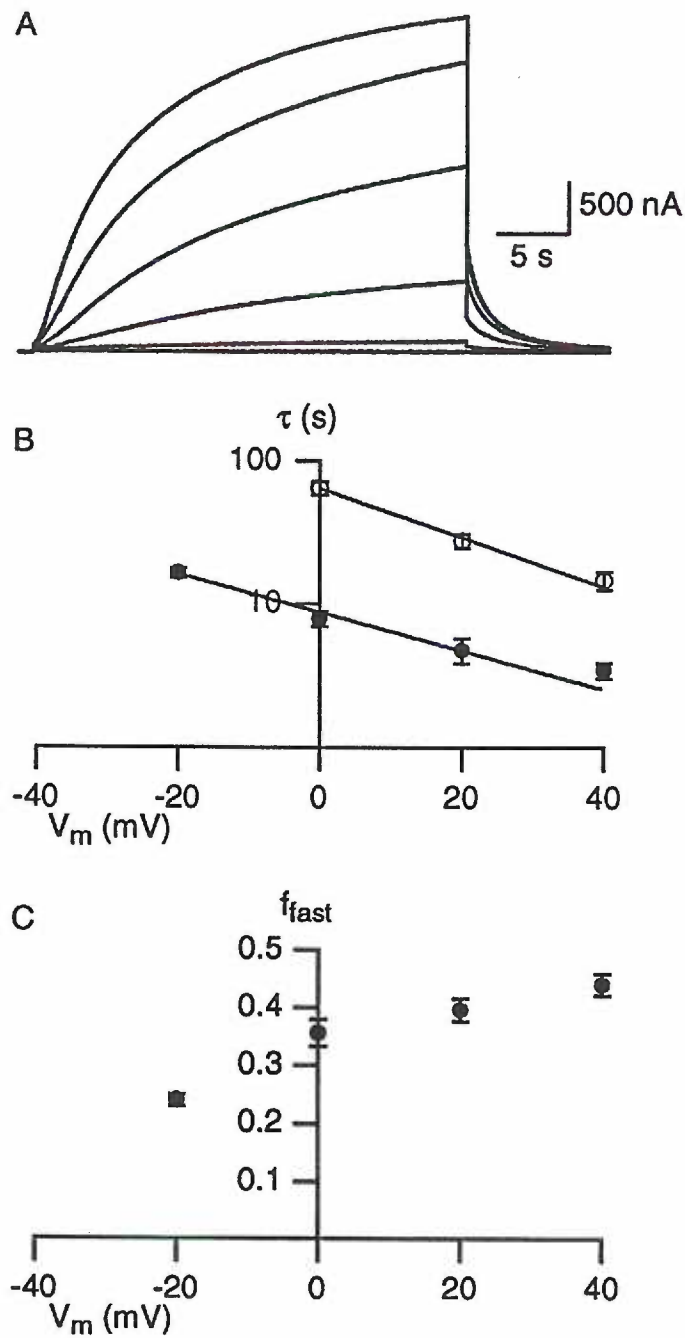
The different structural and functional features of minK suggest a distinct mechanism for voltage-dependent gating. In the experiments described here, we used ionic current measurements to examine the different states that minK channels undergo during gating. The main finding of this study is that the activation of minK channels deviates from the Cole and Moore prediction and can not be explained by a simple sequential gating scheme that involves identical and independent steps. Additionally, reactivation of minK channels is much faster than activation suggesting a potential physiological role for minK channels under conditions that mimic our reactivation protocol. Based on our results we suggest a simple kinetic model in which minK channels reach a common open state through two different pathways.

Activation and deactivation kinetics

Injection of minK mRNA into *Xenopus* oocytes induces voltage-dependent potassium currents which activate with a characteristic, slow time course. Figure V, 1A shows two-electrode voltage clamp recordings of a representative current family evoked by 30s depolarizing commands, from a holding potential of -80 mV to test potentials from -60 to 40 mV. Following depolarization to potentials more positive to -20 mV, the currents show an initial delay prior to activation and the rising phase was well fit by a double exponential. The average time constants for the two processes were plotted as a function of the test potential (fig. V, 1B). Both processes are voltage-dependent and the relative contribution of the fast component increases with more depolarized voltages (fig. V, 1C). The tail currents (fig. V, 1A) show that the time course of deactivation may be faster than activation. Deactivation kinetics were measured by a protocol in which the membrane potential was stepped to 40 mV for 20 s followed by repolarizing test commands to potentials between -20 and -140 mV. For potentials between -20 and -80 mV the tail currents were well fit by the sum of two exponentials while for potentials more negative than -80 mV, single exponential fits were used to describe the deactivation kinetic properties of the currents (fig. V, 2A). The two time constants were plotted as a function of the test tail potential (fig. V, 2B) demonstrating that deactivation is also voltage-dependent and faster than activation.

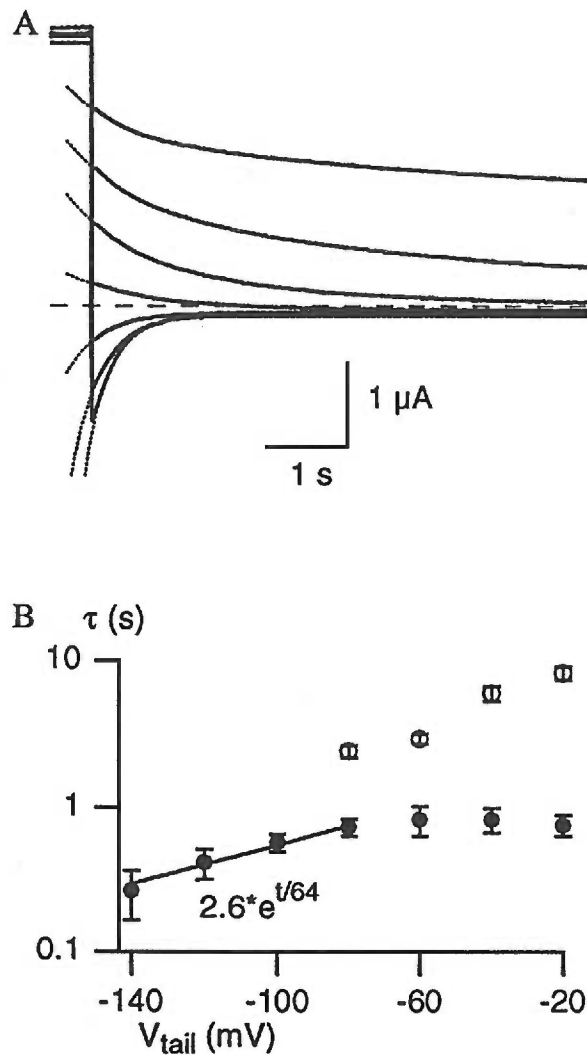
Deviation from the Cole-Moore prediction

The holding potential determines in which state the channel resides, the more depolarized, the closer the channel resides to the open state. Therefore, the effect of holding potential on the time course of minK activation was examined. Figure, V, 3A shows current traces recorded from a single oocyte at 40 mV from holding potentials varying from -60 to -120 mV. As the holding potential was made more positive, the delay associated with the onset of the current decreased. However, the current traces



Figure, V, 1. Activation kinetics of minK channels. Current records from oocytes expressing minK channels (A), time constants of activation plotted as function of the test potential (B), relative amplitude of the fast component plotted against voltage (C). From a holding potential of -80 mV, currents were elicited by 30-s depolarizing commands to potentials

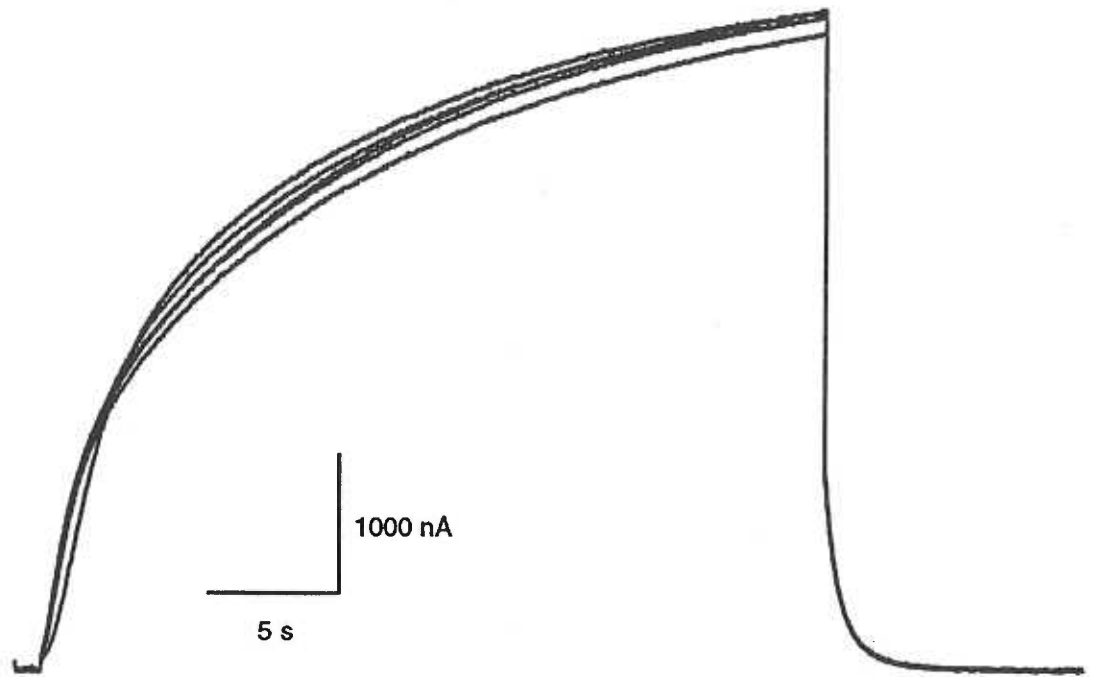
from -60 to 40 mV in 20-mV increments followed by repolarization to a tail potential of -60 mV. Time constants for activation were derived by fitting a sum of two exponentials to the rising phase of the current traces.



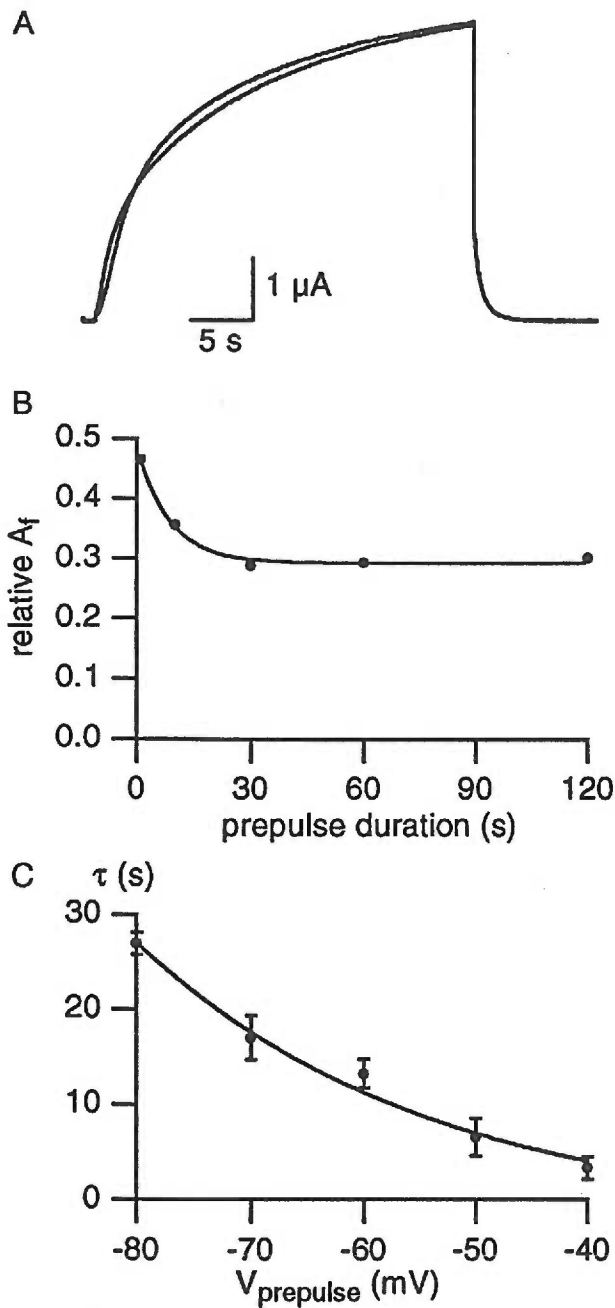
Figure, V, 2. Deactivation kinetics of minK channels. Tail currents from oocytes expressing minK channels (A), time constants of deactivation plotted as function of the test potential (B). From a holding potential of -80 mV cells were activated to 40 mV for 20-s and then were repolarized to tail potentials from -20 to -140 mV in 20-mV increments. For potentials between -20 and -80 mV the tail currents were well fit by the sum of two exponentials while for potentials more negative than -80 mV, single exponential fits were used to describe the deactivation kinetic properties of the currents.

crossed each-other (crossover-effect) indicating a change in the activation pathway at the different holding potentials. If the initial delay reflects the time required to transit closed states prior to opening, then the loss of the delay at more depolarized holding potentials may represent channels in closed states closer to the open state. Upon subsequent depolarization the channels undergo fewer conformational transitions before opening. Such an interpretation is consistent with observations first made by Cole and Moore for the squid giant axon potassium current (Cole and Moore, 1960). However, Cole-Moore theory predicts that if the gating mechanism involves sequential transitions through independent closed states, then the current traces obtained at a single test potential from different holding potential should superimpose when shifted along the time axis to an extent equal to the decreased delay. However, the minK currents traces presented in fig. V, 3 crossover each other and do not overlay. This result suggests that minK gating cannot be explained by a simple sequential model of independent and identical, first order transitions between closed states.

To examine the crossover effect more closely, current traces obtained at 40 mV, from holding potentials of either -60 or -120 mV were fit with two exponentials (fig. V, 4A). The time constants were not different ($\tau_{fast(-120)}=3.7\pm 0.43s$, $\tau_{fast(-60)}=3.6\pm 0.38s$ and $\tau_{slow(-120)}=14.7\pm 1s$, $\tau_{slow(-60)}=13.9\pm 1s$) but the relative contribution of the fast component was greater at the more hyperpolarized holding potential ($0.44\pm 0.02s$ at -120 mV and $0.28\pm 0.01s$ at -60mV). One possible explanation is that activation of minK channels may proceed through kinetically distinct pathways and the distribution of channels between each pathway is determined by the holding potential. The two time constants may represent the two separate activation pathways, the fast component being the rate limiting step in one pathway while the slow component is the rate limiting step in the other pathway. This hypothesis predicts voltage dependent transitions between the two alternate pathways. To quantify the effect of holding potential on the



Figure, V, 3. Effect of holding potential on minK current activation. Currents elicited by depolarization to 40 mV coming from holding potentials between -60 and -120 mV in 20 mV increments (A).



Figure, V.4. Time and voltage dependence of the effect of holding potential on minK current activation. Currents elicited by depolarization to 40 mV coming from holding potentials of -60 and -120 mV (A). The rising phase of the current was fit by a double exponential and the relative amplitude of the fast time constant was plotted as a function of the prepulse duration (B). These data were well described by a single exponential, yielding

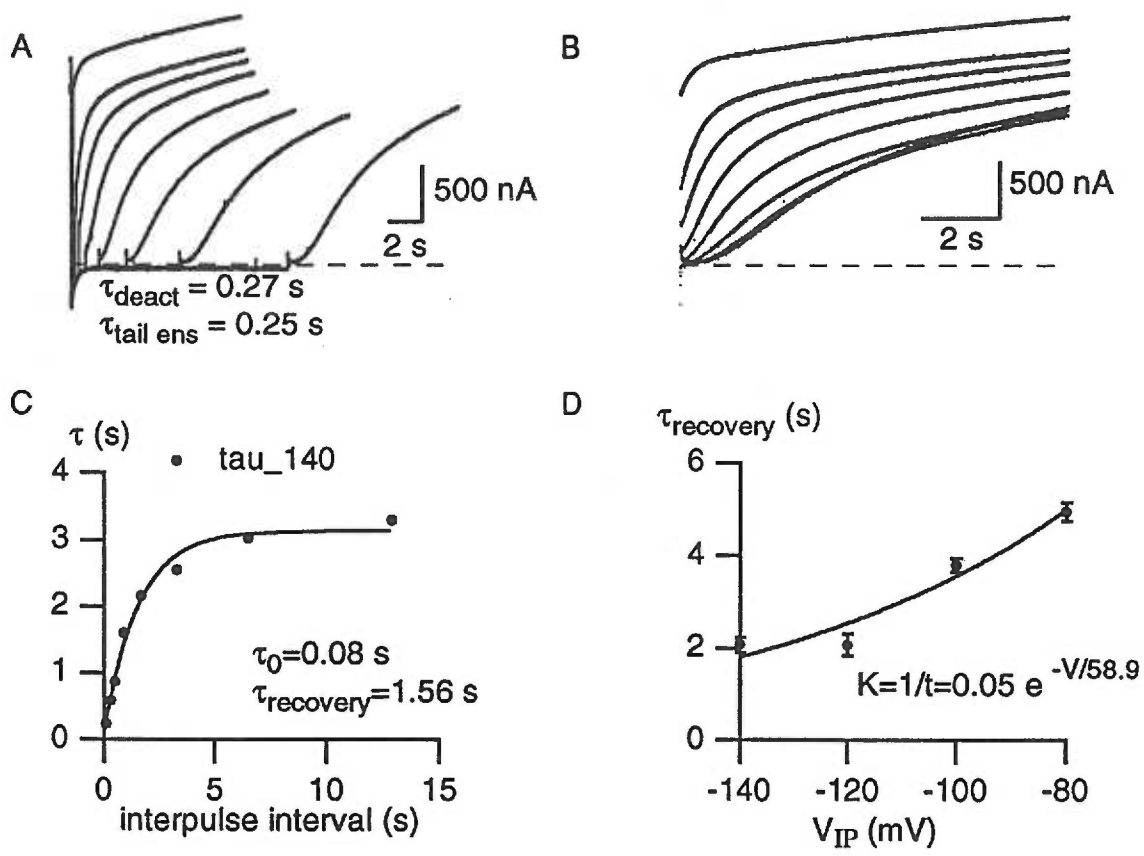
a time constant for the crossover at 60 mV. Similar experiments were performed for prepulse potentials between -100 and 50 mV, the time constant derived for each prepulse potential was plotted as a function of the prepulse potential (C). These data were well described by a single exponential, demonstrating that the partitioning between the two different states is voltage dependent.

distribution of the channels between the alternate pathways the changes in the relative contribution of the fast component were examined as a function of the holding potential. From a holding potential of -100 mV, a prepulse to -60 mV was applied for a varying period of time prior to a command to 40 mV. The rising phase of the current was fit with a double exponential and the relative amplitude of the fast time constant plotted as a function of the prepulse duration (fig.V, 4B). These data were well described by a single exponential, yielding a partitioning time constant of 13.25 ± 1.5 s at 60 mV. Similar experiments were performed for prepulse potentials between -90 and -50 mV, while the holding potential was -100mV. The time constants calculated for the different potentials were plotted as a function of the prepulse potential. These data were well described by a single exponential, demonstrating that the partitioning between the two different states is voltage dependent (fig.V, 4C). To look at the voltage dependence of the reverse process, cells were held at -50 mV and a prepulse to a voltage range between -100 and -60 mV was applied for varying amount of time prior to a command to 40 mV. Similar analysis was performed as for figures V, 4A and 4B and the time constant for the reverse transition was plotted as a function of the prepulse voltage (data not shown).

Recovery from deactivation

The results show that changes in the holding potential shift minK channels into different closed states. This shift most likely represents transition between closed states most removed from the open state. To evaluate closed states near the open state, experiments to measure reactivation following brief closures were performed. The membrane was stepped to 40 mV for 15 s and then back to -140 mV (interpulse voltage) for varying durations (interpulse interval) prior to a return to 40 mV; the time course of reopening was assessed (figure, V, 5A). The kinetics of reopening were

assessed by fitting the sum of two exponentials to the rising phase of activation. The time constant of the fast component was plotted as a function of the interpulse duration (figure, V, 5C). These data were well fit by a single exponential, yielding a time constant for the recovery from deactivation for each voltage. This analysis was performed for interpulse voltages (-140 to -80 mV). The time constants derived by the analysis just described were plotted as a function of the interpulse voltage. These data were fit with a single exponential, revealing the voltage dependence for the recovery from deactivation (figure, V, 5D). Figures V, 5A and B (same as in (A) but traces are shifted along the time axis, so that they start at the same time point) show that as the interpulse interval at -140 mV was increased, the lag prior to activation became more pronounced, suggesting that when allowed to deactivate for longer periods of time at this very negative potential, the channels progress to closed states more distant from the open state and must undergo multiple transitions before reopening. As for activation, Cole-Moore theory predicts that a gating mechanism with any number of independent and identical transitions will follow the same time course of reactivation with a simple shift along the time axis as the duration of the interpulse interval is varied. However, as for activation, minK reactivation is inconsistent with Cole-Moore behavior; the traces do not overlay when shifted along the time axis (figure, V, 5B). Note also, that unlike the predictions for an independent scheme, the currents become appreciably sigmoidal well before deactivation is complete (figure, V, 5A). In addition, the sigmoidicity keeps on becoming more pronounced, the longer the interpulse interval before reactivation, although the channels have completely deactivated. Same is true for the fast time constant of reactivation, it continues on getting slower, although the channels have completely deactivated. Thus, the kinetics of recovery from deactivation provide information for transitions between close states before the close state, (deactivated state), preceding the open state.



Figure, V, 5. Recovery from deactivation. The membrane was stepped to 40 mV for 15 s and then back to -140mV (interpulse voltage) for varying durations (interpulse interval) prior to a return to 40 mV; the time course of reactivation was assessed (A). Traces from (A) are shifted along the time axis, so that they start at the same time point (B). The tau fast of reopening is plotted as a function of the interpulse interval, for interpulse voltage of -140mV (C) . The taus describing the time dependence for recovery from deactivation for different intrpulse voltages are plotted as a function of the interpulse voltage. These data were fit with a single exponential, demonstrating the voltage dependence of recovery from deactivation.

Voltage dependence of reactivation

The voltage protocol employed in figure, V, 5 determined the distribution of channels between the different closed states. Next, a protocol was used which deactivated a constant percentage of channels and the voltage-dependence of reactivation was assessed. Channels were activated by a 20 s pulse to 40 mV from a holding potential of -80 mV. Then, a fraction of the channels, (~16 %) were closed by a brief (100 ms) hyperpolarizing pulse to -140 mV, followed by depolarizing commands to test potentials between -40 and 40 mV (fig. V, 6A). The rising phase of reactivation was fit with a double exponential, and the fast time constant was plotted as a function of the test potential, showing that reactivation is only slightly voltage-dependent between -40 and 40 mV (fig. V, 6B). The brevity of the interpulse interval assures that the deactivated channels reside in closed states close to the open state.

Deactivation kinetics do not reveal more than one, kinetically different, open state

The results described above examine the different closed states during minK gating. To determine whether the channels may enter kinetically distinct open states, the effect of the duration of the test pulse and of the holding potential on deactivation kinetics was examined. Traces evoked by depolarizing commands to 40 mV for varying durations, from a holding potential of either -120 or -60 mV, are shown in figure, V, 7A and B, respectively. From a holding potential of either -60 or -120 mV, repolarization from 40 mV to -60 mV deactivated the channels with similar time courses. Figures, V, 7C and D show the time constants of deactivation plotted as a function of the holding potential and the duration of the test pulse. The similar time constants show that the channels deactivate from a kinetically indistinguishable open state.

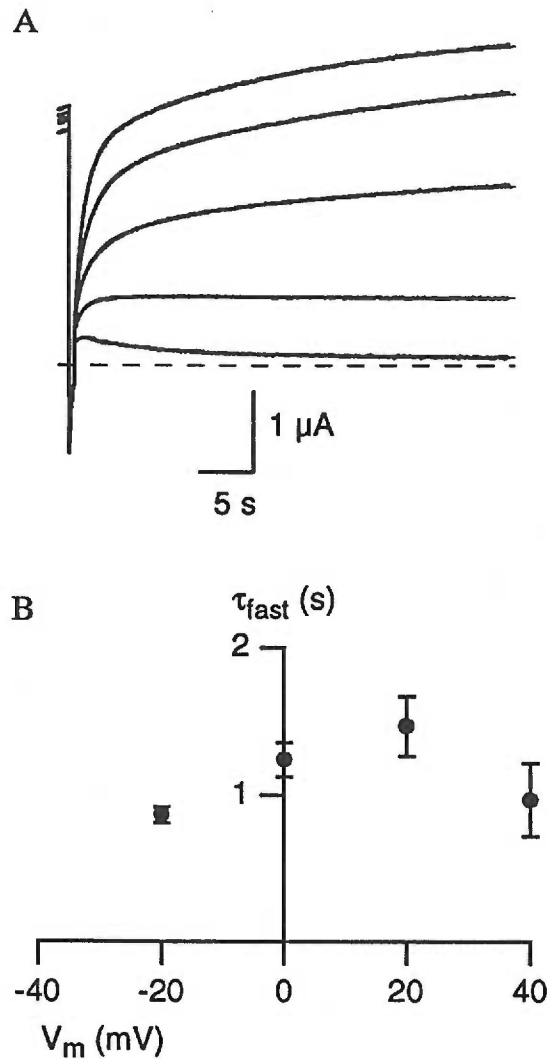
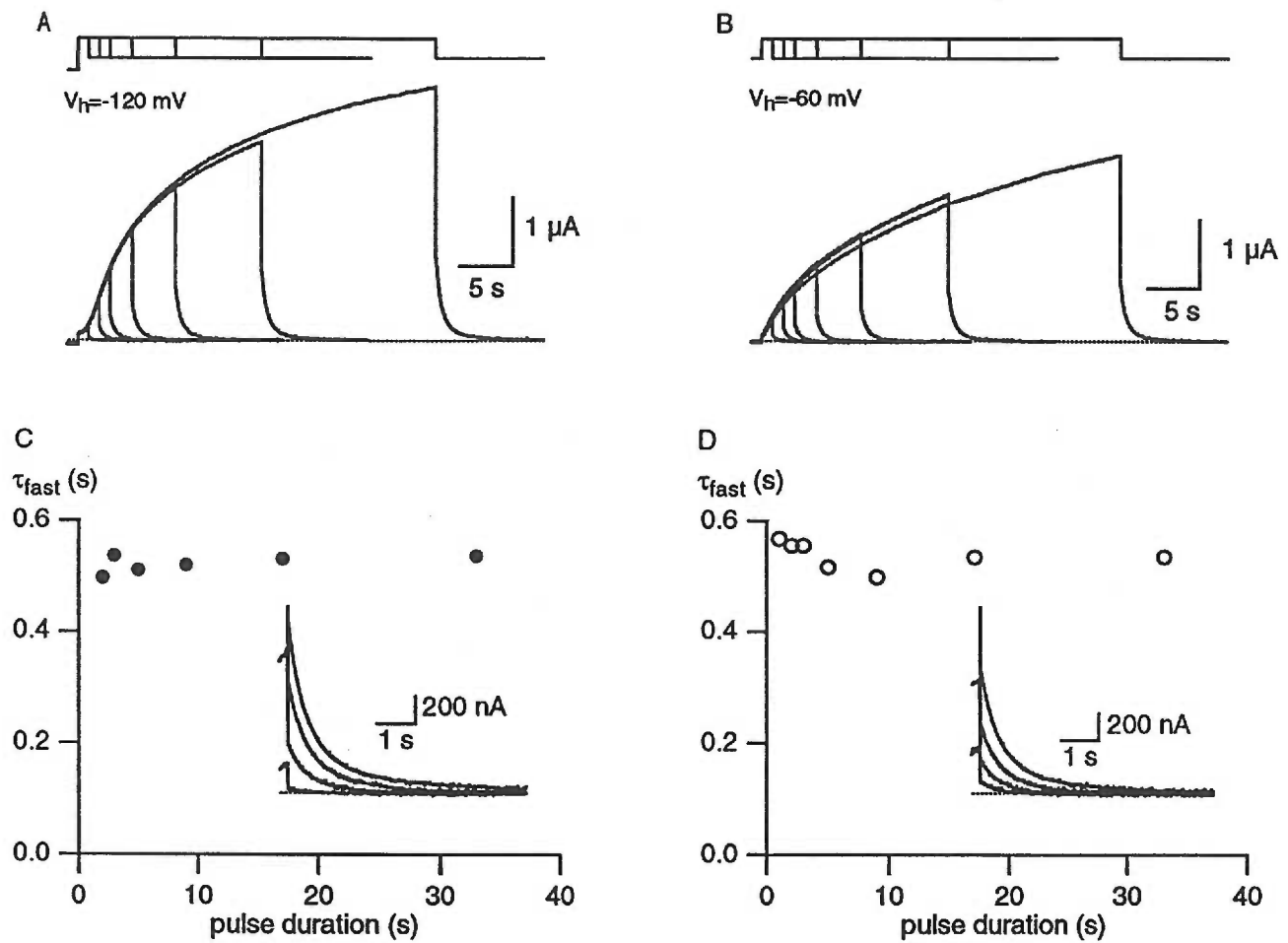


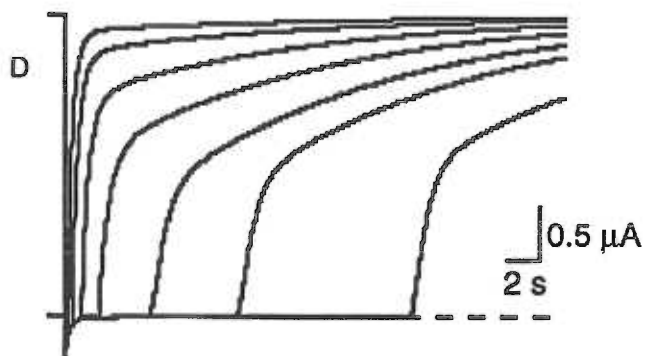
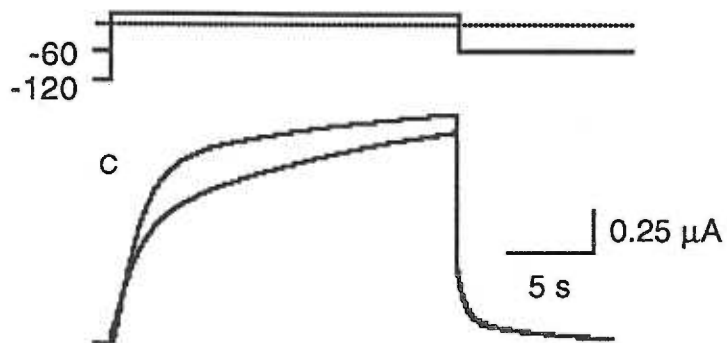
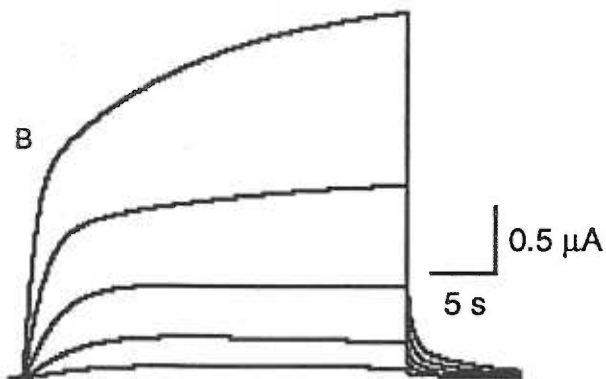
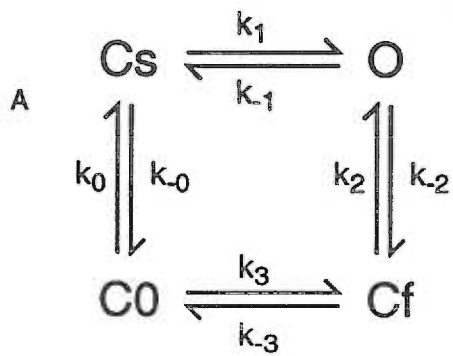
Figure V.6. Kinetics of reactivation. Channels were activated by a 20 s pulse to 40 mV from a holding potential of -80 mV. Then, a fraction of the channels, (~16 %) were closed by a brief (500 ms) hyperpolarizing pulse to -140 mV, followed by depolarizing commands to test potentials between -40 and 40 mV (A). The voltage-dependence of reactivation was examined by fitting the rising phase of reactivation with a double exponential, and the fast time constant was plotted as a function of the test potential (B).

Taken together these results demonstrate that gating of minK channels can not be explained by a sequential model that involves identical and independent steps. Alternatively, it may be most simply modeled by a gating scheme in which minK channels reach a common open state through two different pathways (fig., V, 8A). When the membrane is held at more hyperpolarized potentials, such as -140 mV, minK channels reside primarily in C0 and may activate through Cf, a relatively faster pathway, prior to the open state. At less negative potentials such as -60 mV, minK channels transit through Cs, a slower pathway, prior to reaching the open state. The transition between C0 and Cs describes the crossover effect.

The transition between Cs and O describes the activation of minK channels through the slow pathway; leaving a holding potential of -60 mV, while the transition between C0 and Cf represents the activation of minK channels through the fast pathway; leaving a holding potential of -140 mV. Deactivation kinetics represent the transition between O and Cf, while reactivation kinetics are describing the reverse transition. Finally, kinetic information derived from the recovery from deactivation provided information for the transition between Cf and C0. The rate constants for the transitions are given in table V 1, and in all cases, except for k_{-1} , they were calculated based on the experimental data. We let k_{-1} floating, so that the product of forward constants equals the product of backward constants. Figures V 8B, C and D show computer simulations of the kinetic properties of minK currents based on our model. The model, successfully, reproduces the slow time course of current activation and deactivation, (figure, V, 8B), the crossover of the currents as a function of the holding potential, (figure, V, 8C), the fast reactivation kinetics and the recovery from deactivation (figure, V, 8D).



Figure, V, 7. Envelope of tails. Traces evoked by depolarizing commands to 40 mV for varying durations, from a holding potential of -120mV(A) or -60 mV (B). The time constant of deactivation plotted as a function of prepulse duration (C),(D). Tail currents were measured at -80 mV.



Figure, V, 8. State model and computer simulations of minK currents.

Mink channels reach a common open state through two different pathways (A). The simulated currents in (B) show a family of current traces between -40 and 40 mV, with 20 mV increments. Tail currents were obtained at -60 mV. The simulated currents in reproduce the deviation from Cole-Moore prediction, (C), and the recovery from deactivation (D). The protocol in (D) is the same as in fig., V, 5A.

Table V, 1: Rate constants for the transitions describing the state model

$$k_0 = 0.3 * e^{V/30}$$

$$k_{-0} = 0.015 * e^{-V/60}$$

$$k_1 = 0.01 * e^{V/30}$$

$$k_2 = 0.6 * e^{-V/64}$$

$$k_{-2} = 1.5 * e^{V/60}$$

$$k_3 = 0.06 * e^{-V/50}$$

$$k_{-3} = 0.1 * e^{V/27}$$

$$k_{-1} = k_0 * k_1 * k_2 * k_3 / (k_{-0} * k_{-2} * k_{-3})$$

Conclusions

Based on ionic current measurements, we concluded that the kinetic behavior of minK channels deviates from the Cole and Moore prediction, and can not be described by an independent gating scheme that involves identical, independent steps. Alternatively, we suggest that, unlike other voltage-gated K^+ channels, minK channels reach a common open state through two different pathways.

In addition, reactivation of minK channels is much faster than activation, suggesting a potential role of minK in the maintenance of regular heart rate in cardiac cells, under physiological conditions that mimic the reactivation protocol, such as early after depolarizations (for more details see, discussion, chapter VI).

CHAPTER VI

Description, discussion and conclusions

In science, like in everything else, it is relatively easy to describe and to discuss while it is quite difficult to conclude. However, people (e.g., reviewers, professors, parents, etc.) need conclusions, because conclusions give answers (true or false, if that matters), and answers are important for any system in order to justify its existence and to evolve.

Is minK a channel, does it require additional subunits or is it a channel regulator?

The currents elicited by expression of the minK protein in *Xenopus* oocytes display properties characteristic of K⁺ channels, including voltage-dependent gating, ion selectivity, and blocker pharmacology. However, because of its distinct structure, it is not yet clear whether the minK protein is a K⁺ channel-forming subunit or whether it acts as a regulator of endogenous, otherwise silent channels.

Attali (Attali, 1993) reported that high levels of expression of the minK protein in *Xenopus* oocytes resulted in both a potassium and a chloride current. The K⁺ and Cl⁻ currents were distinguished by their pharmacological and regulatory profiles. In addition mutations were found in the minK protein which selectively abolished either the chloride channel activity or the potassium channel activity. These results were interpreted as demonstrating that the minK protein is not a channel-forming protein, but

rather an inducer of otherwise silent oocyte channels. However, the hyperpolarization-activated current observed by Attali (Attali, 1993) is pharmacologically indistinguishable from that which is seen following high levels of expression of five structurally and functionally distinct membrane proteins (chapter III). Based on our data, mutations in the minK protein which abolish chloride activity but retain potassium channel activity form functional minK channels, but are reduced in their levels of minK protein expression, such that they do not activate the hyperpolarization-activated current (see chapter III). On the other hand, mutations which abolish potassium channel activity and retain chloride channel activity form non-conducting minK channels, but which express high enough levels of protein to induce the endogenous hyperpolarization-activated current. Therefore, the data presented by Attali are based on experimental artifacts and do not address the issue of whether the minK protein forms an ion channel. However, several studies have provided strongly suggestive evidence that the minK protein is a pore-forming subunit.

The finding that specific mutations of the minK protein influence the characteristics of the induced current strongly suggests that the minK protein is part of the channel pore, rather than being an indirect activator of some other endogenous channel protein. Mutagenesis of amino acids within the TM region produced changes in permeation and pharmacology. Changes in ionic selectivity were induced by mutation of a phenylalanine at position 55 in the TM into smaller residues such as threonine or alanine. Goldstein and Miller (1991) found that mutation of a phenylalanine at position 55 in the TM into alanine (F55A) produced channels that were approximately three times more permeable to ammonium and cesium ions than the wild-type channels. The same mutation resulted in currents that were more sensitive to blockade by TEA and cesium.

Moreover, Wang (Wang et al., 1996) used scanning cysteine accessibility mutagenesis and identified three residues in the TM that when mutated to cysteines rendered minK

channels sensitive to irreversible block by methanethiosulfonateethylsulfonate (MTSES). These data support the hypothesis that minK is a pore-forming subunit and neither support nor exclude the possibility that minK associates with other subunit(s) to form functional K⁺ channels.

Several pieces of evidence suggest that the minK protein interacts with additional(s) protein(s) to form functional channels. Different from other cloned K⁺ channels, heterologous expression of minK currents has, so far, been limited to oocytes and HEK293 cells, a human embryonic kidney cell line (Freeman and Kass, 1993). Moreover, the amplitude of minK currents saturates after injection of only 1ng of minK mRNA (Blumenthal and Kaczmarec, 1994) while the amplitudes of currents obtained by expression of other cloned K⁺ channels are, in general, proportionate to the amount of injected mRNA. To account for these observations it has been proposed that the minK protein needs an auxiliary protein to form functional channels. The identity or even the existence of such a protein remains unproved, but possibilities include a cytoskeletal element, a regulatory protein, or another subunit that contributes structurally to the pore of the channel. Such a protein must be present in oocytes and HEK 293 cells but not other cells.

Additional evidence to support the hypothesis that the minK protein interacts with some endogenous oocyte or HEK 293 protein to generate functional channels has also come from the cloning of another protein, termed CHIF (channel-inducing factor), unrelated in primary sequence to the minK protein (Attali et al., 1995). When injected into oocytes, the mRNA for this protein, induces currents that resemble minK currents in all physiological and pharmacological characteristics, including its sensitivity to clofilium, phorbol esters, cyclic AMP and intracellular calcium changes.

Taken together, the data from mutagenesis studies, expression of different levels of the minK protein, and in different expression systems support the hypothesis that the minK

protein is a pore-forming subunit which requires additional(s) factor(s) to generate functional channels.

Structural composition of minK channels

A great deal has been learned about the assembly and structural composition of cloned potassium channels, except for minK. Because of the dramatically different structure of the minK protein, it is unclear how the minK protein might form a potassium channel. To determine whether minK channels are comprised of more than one monomer, and to estimate the subunit stoichiometry of minK channels, the difference in voltage dependence and kinetics between wild type and S69A channels were exploited. Injecting a constant amount of wild type mRNA with increasing amounts of S69A mRNA led to decreased potassium currents at all potentials tested, suggesting that the two different kinds of subunits coassemble. In addition, the kinetics of the current at -20 mV are indistinguishable from wild type, while at more depolarized potentials the kinetics are not consistent with channels comprised only of wild type or S69A subunits. Thus, injection of mixtures of wild type and S69A mRNAs results in a heterogeneous population of channels with relative proportions reflecting a binomial distribution, and the exponent equal to the subunit stoichiometry of the channel. At -20 mV only the subpopulation comprised of all wild type subunits can pass ions. Application of the binomial distribution to the decrease in wild type tail current amplitudes following commands to -20 mV, yielded a value of 14 minK monomers per functional minK channel. This result is based on three assumptions. The first assumption is that wild type and mutant channels express equally. Takumi et al., 1991, used immunoprecipitations to determine the relative amount of wild type and S69A subunits in *Xenopus* oocyte membranes and found little if any difference. The second assumption is that wild type and mutant subunits assemble randomly. This is

supported by the data from oocytes injected with equal amounts of wild type and S69A mRNAs; at -20 mV no current was detected. If wild type or S69A subunits more readily formed homo- rather than heteromeric complexes, then some wild type channel activity would be expected. Further, identical estimates for minK subunit stoichiometry were obtained using F55A, a mutation residing within a different region of the subunit. The third assumption is that only homomeric wild type channels pass current at -20 mV; one or more S69A subunits alter channel function such that they cannot pass current at this potential. This is suggested by the finding that regardless of the amount of S69A mRNA coinjected with wild type mRNA, the activation and deactivation rates, and the voltage-dependence of currents elicited at -20 mV are indistinguishable from wild type. Further, the data points are best fit when constrained to this assumption. The fit is much poorer when modified to assume that two or more S69A subunits are required to alter channel function. If two or more S69A subunit are required, then the coefficient, n , would necessarily become larger and the number of subunits per functional minK channel would increase (Figure, IV, 3f). For instance, if two S69A subunits are required for inhibition at -20 mV then the subunit stoichiometry would be 26; this is not compatible with the data. However, we cannot exclude that one S69A subunit may cause partial inhibition while two result in complete inhibition; n would then be between 14-36 (see below).

Using a similar approach, Wang et al., 1995 have estimated a much smaller number of minK monomers in a functional channel. These workers co-expressed wild type minK with a point mutant (D77N) which yields no current in the normal voltage range of activation. When the two different mRNAs are coexpressed in 1:1 ratio, the amplitude of minK current is reduced to approximately one fourth of that resulting from the injection of the same amount of wild type mRNA alone. Using the same analysis and assumptions as we used, their experimental data most closely match a value of two minK monomers per functional channel.

In both studies the quantitative conclusions about the stoichiometry of functional minK channels are based on assumptions that have not been tested directly. However, a larger number than two minK subunits could match the experimental data by Wang et al., 1995, if the assumption that only fully wild type channels pass current is not correct. It might be that complexes containing one or two mutant subunits are able to conduct. If this is true, then the analysis by Wang et al., 1995, would have underestimated the number of minK monomers per functional channel.

The finding that minK channels are comprised of at least 14 subunits is in contrast to the other known potassium channel families in which the subunit stoichiometry is four. The dashed curve in Figure IV, 3e shows the predicted fit if four minK subunits make a functional channel; the data clearly do not support this stoichiometry.

How 14 minK subunits form functional K⁺ channels

How might such a molecule form an ion channel? When channels are formed by identical subunits, it is generally assumed that the subunits have the same conformation and are related by radial symmetry about the axis of the pore. If minK channels are formed by assembly of at least 14 identical subunits, they cannot be arranged with 14-fold radial symmetry because the pore would be too large to accommodate selectivity. We postulate that minK channels assemble in two stages. First, three monomers associate into a trimeric structure with three-fold symmetry in which the TM helices form triple stranded coiled-coils. Each trimer has classic "knobs-into-holes" helix packing, typical of coiled-coils, and each of the subunits occupies an equivalent position.

The channel is hypothesized to form by the assembly of multiple trimers. Although the data are best fit if at least 14 subunits assemble to form minK channels, the packing of the helices is greatly improved if the channel is formed by five trimers, a "pentamer-of-

trimers" with five-fold radial symmetry, in which the pore is formed from five internal subunits surrounded by ten outer subunits (Figure IV, 4a). Because of the symmetry inherent in the trimers, each trimer subunit is equivalently capable of contributing to the formation of the inner ring. In this arrangement four phenylalanine residues (F54, 55, 57, 58) pack tightly together within each coiled-coil and positively charged residues (R68, K70, K71) at the cytoplasmic end of the helices face away from the coiled-coils and interact with lipid head groups. While the helical packing between subunits within the trimers is typical of coiled-coils, the helical interactions between trimers is less typical. The channel is "closed" in this conformation because the central five helices are packed tightly together with positively charged residues near their termini inhibiting cation permeation. Membrane depolarization induces a rearrangement of the helices, as illustrated in Figure IV, 4b; in the open state all adjacent helices pack according to knobs-into-holes theory. The central five helices, those which form the pore, undergo the most dramatic movement during the closed->open conformational change, shifting from a left handed to a right handed spiral around the axis of the pore. Such a conformational change upon gating extends F55 and T59, which have been shown to affect ion selectivity (Goldstein and Miller, 1991), into the pore, and orients charged residues (E44 and E73) toward the pore at either end of the helices.).

Gating mechanism

The different structural and functional features of minK suggest a distinct mechanism for voltage-dependent gating. In the experiments described here (chapter V), we used ionic current measurements to examine the different states that minK channels undergo during gating. The main finding is that the kinetic behavior of minK channels deviates from the Cole and Moore prediction and can not be described by an independent gating scheme that involves identical and independent steps. Alternatively, we suggest a

simple kinetic model in which minK channels reach a common open state through two different pathways.

The different gating mechanism of minK channels is supported by previous crosslinking studies (Varnum et al., 1995) and analysis of the subunit stoichiometry of minK channels (Tzounopoulos et al., 1995). These experiments support a model in which minK channels activate by subunit assembly. According to this model, aggregation of 5 preformed trimers form a pentamer of trimers with five -fold radial symmetry in which the pore is formed from 5 internal subunits, one donated by each trimer. These internal subunits are surrounded by 10 outer subunits (Tzounopoulos et al., 1995). Therefore, the two alternative activation pathways revealed by the present studies might reflect the process of assembly. One pathway may be aggregation of pentamer of trimers, while the other pathway might be direct channel formation by aggregation of 15 independent monomers. The equilibrium between these two alternative pathways is determined by the holding potential.

To explain the dependence of minK gating on the amount of mRNA injected, Cui et al., 1994, proposed three different kinetic models. Although none of these models reproduced the deviation from the Cole-Moore prediction described in our study, inherent to their model is an interaction between minK subunits which modulates channel gating; a higher density of subunits increases this interaction. Both models presented by Cui et al and the model presented here propose a fundamental deviation from a basic tenet of ion channel properties, that each subunit is independent of all others.

The other main finding of our experiments is that reactivation of minK channels is much faster than activation suggesting a potential role for minK channels under physiological conditions that mimic our reactivation protocol.

Mink is remarkable because its activation kinetics are so sensitive to the holding potential and to reactivation conditions. The dependence on holding potential and the fast reactivation kinetics of minK channels may be of physiological significance in heart, as the minK protein is thought to underlie the slow component of the delayed rectifier in cardiac ventricular myocytes. In a normal cardiac action potential, the membrane potential becomes depolarized by the inward flow of Na^+ and Ca^{+2} ions. This depolarization leads to the opening of voltage-dependent K^+ channels and the resulting outward flow of potassium ions resets the membrane potential back to a more negative resting potential. However, sometimes, brief aberrant depolarizations (early "after-depolarizations") occur which tend to trigger an action potential prematurely. Such a depolarization following the falling phase of the cardiac action potential resembles the protocol we used to examine minK channel recovery from deactivation, (fig. V, 6), a long depolarization (plateau phase) followed by a brief repolarization (falling phase), and then a second brief depolarization (early "after-depolarization"). Under these conditions, minK channel activation is accelerated and provides the outward current which suppresses the effects of the unwanted depolarization. Thus, the behavior of minK described here, (fig. V, 6), is just what is needed to guard against such early after-depolarizations.

Endogenous channel activity in *Xenopus* oocytes

Xenopus oocytes are widely employed for expression of foreign proteins, most notably electrogenic molecules such as ion channels and transporters. Among the advantages of the oocyte expression system is the ability to obtain high levels of expression, permitting detailed quantitative analysis of currents essentially free of contaminating endogenous currents. Beginning with Shaker, voltage-gated potassium channels have been expressed and extensively studied in *Xenopus* oocytes using depolarizing voltage protocols (Timpe et al., 1988; Christie et al., 1989; Pongs et al., 1989). More recently,

a new family of potassium channel subunits has been described, the inward rectifiers, and investigation of the structure and function of this family of channels has become a central theme in many laboratories. Inward rectifiers readily pass current at potentials negative to E_K while current is decreased at more positive potentials, therefore hyperpolarizing voltage protocols are employed (Kubo et al., 1993 a, b; Ho et al., 1993; Dascal et al., 1993; Bond et al., 1994). Because of the high levels of channel expression obtained in *Xenopus* oocytes, contributions by endogenous channels to current amplitudes are not considered significant. However, under some circumstances this assumption is incorrect and may lead to erroneous interpretations.

The results presented on chapter III, demonstrate that high levels of expression of many membrane proteins in *Xenopus* oocytes result in the induction of an endogenous hyperpolarization-activated current (Tzounopoulos et al., 1995). In the presence of calcium, the current is comprised of two components, a calcium-activated chloride current and a nonselective cation current; when calcium is eliminated from the extracellular solution, only the nonselective cation current remains. It is possible that the calcium-activated chloride current is induced by calcium flowing into the cell through the nonselective cation channel. The hyperpolarization-activated current does not require extracellular calcium for activation, is blocked by DIDS and TEA, accentuated by clofilium, and is pH-sensitive. The current was occasionally detected in some noninjected oocytes, but high levels of heterologously expressed membrane proteins consistently induced the current, while in oocytes expressing moderate levels the current was either not detectable or present only in some oocytes.

Although the amount of membrane proteins were not specifically quantified, we assume that longer time after injection of a constant amount of mRNA is correlated with higher levels of expression. For electrogenic molecules this is clearly seen as a correlation

between time after injection and current amplitudes. As shown in figure III, 4, gating charge, presumably reflecting the number of channels on the oocyte surface, was quantitatively correlated with the appearance of the hyperpolarization-activated current. Therefore, it is important to examine currents elicited by hyperpolarizing protocols for contamination by this endogenous current. The dependence of the tail current reversal potential on external calcium and the distinct pharmacology of the current serve as defining characteristics which distinguish the endogenous hyperpolarization-activated current from those arising from heterologously expressed proteins.

Summary and future directions

In the absence of most *direct* approaches to address the main questions concerning the minK protein, studies such as those described in this dissertation are the best available methods to address the structure and function of minK channels.

Our studies refuted the data underlying the model in which the minK protein acts as a regulator of endogenous, otherwise silent channels. Additionally, we provided an estimate of 14 minK subunits per functional channel, suggesting a structural model for minK channel formation. Finally, we concluded that minK gating can not be described by a scheme that involves identical and independent steps. Alternatively, we suggest that, unlike other voltage-gated K⁺ channels, minK channels reach a common open state through two different pathways.

The present data from our studies and those of other investigators suggest that the minK protein forms the pore of a potassium channel, perhaps in conjunction with another, as yet, unidentified protein. The unique structure of minK is reflected in (by) its unique mechanism of channel formation and gating. While no experiment is conclusive in itself, the combined efforts of many groups have provided a relatively

sophisticated understanding of minK structure, function and gating but most importantly have set the frame for future more direct studies.

The future minK investigations must address the identification of the hypothesized co-factor(s), and a biochemical determination of the subunit stoichiometry (immunoprecipitations from myocytes or heterologously expressing minK cells). Such experiments will provide conclusive answers to the central questions of minK structure. Finally, efforts towards the crystallization of the minK protein will shed real light on the structure of the minK protein and the assembly of minK monomers into functional channels.

REFERENCES

Adelman, J. P., Shen, K. Z., Kavanaugh, M. P., Warren, R. A., Wu, Y. N., Lagrutta, A., Bond, C. T., and North, R. A. (1992). Calcium-activated potassium channels expressed from cloned complementary DNAs. *Neuron* 9, 209-216.

Armstrong, C. M., and Bezanilla, F. (1973). Movement of sodium ions associated with the nerve impulse. *Nature* 242, 457-461.

Arriza, J. L., Fairman, W.A., Wadiche, J.I., Murdoch, G.H., Kavanaugh, M P., Amara, S.G. (1994). Functional comparisons of three glutamate transporter subtypes cloned from human motor cortex. *J. of Neuroscience* 14, 5559-5569.

Attali, B., Guillemare, E., Lesage, F., Honore, E., Romey, G., Lazdunski, M., Barhanin, J. (1993). The protein IsK is a dual activator of K⁺ and Cl⁻ channels. *Nature* 365, 85-852.

Attali, B., Romey, G., Honore, E., Schmid-Alliana, A., Mattei, M.-G., Lesage, F., Ricard, P., Barhanin, J., and Lazdunski, M. (1992). Cloning, functional expression, and regulation of two K⁺ channels in human T lymphocytes. *J. Biol. Chem.* 267, 8650-8657.

Bezanilla, F., Perozo, E., and Stephani, E. (1994). Gating of Shaker K⁺: II. The components of gating currents and a model of channel activation. *Biophys. J.* *66*, 1011-1021.

Blumenthal, E. M., and Kaczmarek, L. K. (1993). Inward rectification of the MinK potassium channel. *J. Membrane Biol.* *136*, 23-29.

Blumenthal, E. M., and Kaczmarek, L. K. (1994). The minK potassium channel exists in functional and nonfunctional forms when expressed in the plasma membrane of *Xenopus* oocytes. *J. of Neuroscience* *14*, 3097-3105.

Blumenthal, E. M., and Kaczmarek, L. K. (1992). Modulation by cAMP of a slowly activating potassium channel expressed in *xenopus* oocytes. *J. of Neuroscience* *12*, 290-296.

Bond, C. T., Pessia, M, Xia, X.M., Lagrutta, A, Kavavnaugh, M.P., Adelman, J.P. (1994). Cloning and expression of a family of inward rectifier potassium channels. *Receptors and Channels* *2*, 183-191.

Boyle, M. B., MacLusky, N. J., Naftolin, F., and Kaczmarek, L. K. (1987). Hormonal regulation of K⁺-channel messenger RNA in rat myometrium during oestrus cycle and in pregnancy. *Nature* *330*, 373-375.

Bunzow, J. R., Van Tol, H. H. M., Grandy, D. K., Albert, P., Salon, J., Christie, M., Machida, C. A., Neve, K. A., and Civelli, O. (1988). Cloning and expression of a rat D₂ dopamine receptor cDNA. *Nature* *336*, 783-787.

Busch, A. E., Kavanaugh, M. P., Varnum, M. D., Adelman, J. P., and North, R. A. (1992). Regulation by second messengers of the slowly-activating, voltage-dependent potassium current expressed in *Xenopus* oocytes. *J. Phys. (Lond)* 450, 455-468.

Busch, A. E., Varnum, M. D., North, T. A., and Adelman, J. P. (1992). An amino acid mutation in a potassium channel that prevents inhibition by proteinKinase C. *Science* 255, 1705-1707.

Butler, A., Wei, A., Baker, K., and Salkoff, L. (1989). A family of putative potassium channel genes in drosophila. *Science* 243, 943-947.

Christie, M. J., Adelman, J. P., Douglass, J., and North, R. A. (1989). Expression of a cloned rat brain potassium channel in *Xenopus* oocytes. *Science* 244, 221-224.

Christie, M. J., North, R. A., Osborne, P. B., Douglass, J., and Adelman, J. P. (1990). Heteropolymeric potassium channels expressed in *Xenopus* oocytes from cloned subunits. *Neuron* 2, 405-411.

Cole, K. S., and Moore, J. W. (1960). Potassium ion current in the squid giant axon. *Biophys. J.* 1, 161-202.

Cui, J., Kline, R. P., Pennefather, P., and Cohen, I. S. (1994). Gating of IsK expressed in *Xenopus* oocytes depends on the amount of the mRNA injected. *J. Gen. Phys.* 104, 87-105.

Dascal, N., Lim, N. F., Schreibmayer, W., Wang, W., Davidson, N., and Lester, H. A. (1993). Expression of an atrial G-protein-activated potassium channel in *Xenopus* oocytes. *Proc. Natl. Acad. Sci. USA* 90, 6596-6600.

Doerr, T., Denger, R., Doerr, A., and Trautwein, W. (1990). Ionic currents contributing to the action potential in single ventricular myocytes of the guinea pig studied with action potential clamp. *Eur. J. Phys.* 416, 230-237.

Folander, K., Smith, J. S., Antanavage, J., Bennett, C., Stein, R. B., and Swanson, R. (1990). Cloning and expression of the delayed-rectifier I_{sK} channel from neonatal rat heart and diethylstilbestrol-primed rat uterus. *Proc. Natl. Acad. Sci. USA* 87, 2975-2979.

Freeman, L., and Kass, R. S. (1994). Non-stationary fluctuation analysis of K^+ current in guinea pig sinoatrial node and transfected cells and transfected HEK-293 cells. *Biophys. J.* 66, A:143.

Freeman, L. C., and Kass, R. S. (1993). Expression of a minimal K^+ channel protein in mammalian cells and immunolocalization in guinea pig heart. *Circ. Research* 73, 968-973.

Goldstein, S. A. N., and Miller, C. (1991). Site-specific mutations in a minimal voltage-dependent K^+ channel alter ion selectivity and open-channel block. *Neuron* 2, 403-408.

Hille, B. (1992). *Selective permeability: independence.*, second Edition, B. Hille, ed. (Sunderland, MA: Sinauer Associates Inc.).

Ho, K., Nichols, C. G., Lederer, W. J., Lytton, J., Vassilev, P. M., Kanazirska, M. V., and Hebert, S. C. (1993). Cloning and expression of an inwardly rectifying ATP-regulated potassium channel. *Nature* 362, 31-37.

Holsinger, L. J., and Lamb, R. A. (1991). Influenza virus M₂ integral membrane protein is a homotetramer stabilized by formation of disulfide bonds. *Virology* 183, 32-43.

Honore, E., Attali, B., Lesage, F., Barhanin, J., and Lazdunski, M. (1992). Receptor-mediated regulation of IsK, a very slowly activating, voltage-dependent K⁺ channel in xenopus oocytes. *Biochemical and Biophysical Research communications*. 184, 1135-1141.

Honore, E., Attali, B., Romey, G., Heurteaux, C., Ricard, P., Lesage, F., Lazdunski, M., and Harhanin, J. (1991). Cloning, expression, pharmacology and regulation of a delayed rectifier K⁺ channel in mouse heart. *EMBO J* 10, 2805-2811.

Honore, E., and Lazdunski, M. (1991). Hormone-regulated K⁺ channels in follicle-enclosed oocytes are activated by vasorelaxing K⁺ channel openers and blocked by antidiabetic sulfonylureas. *Proc. Natl. Acad. Sci. USA* 88, 5438-5442.

Hume, J. R., and Uehara, A. (1985). Ionic basis of the different action potential configurations of single guinea-pig atrial and ventricular myocytes. *J. Phys.* 368, 525-544.

Iwai, M., Masu, M., Tsuchida, K., Mori, T., Ohkubo, H., and Nakanishi, S. (1990). Characterization of gene organization and generation of heterogeneous mRNA species of rat I_{SK} protein. *J. Biochem.* *108*, 200-206.

Je Zhang, Z., Jurkiewicz, N. K., Folander, K., Lazarides, E., Salata, J., and Swanson, R. (1994). K^+ currents expressed from the guinea pig cardiac IsK protein are enhanced by activators of proteinKinase C. *Proc. Nat. Acad. Sci. USA* *91*, 1766-1770.

Kaczmarek, L. K. (1991). Voltage-dependent potassium channels: MinK and *Shaker* families. *Nature* *350*, 229-230

Ketchum, K. A., Joiner, W. J., Sellers, A. J., Kaczmarek, L. K., and Goldstein, S. A. N. (1995). Primary structure and expression of a new family of potassium channel proteins with two pore domains in tandem. *Nature* *376*, 690-695.

Kowdley, G. C., Ackerman, S.J., John, J.E., Jones, L.R., Moorman, J.R. (1994). Hyperpolarization-activated chloride currents in *Xenopus* oocytes. *J. Gen. Physiol.* *103*, 217-230.

Kubo, Y., Baldwin, T.J., Jan, Y.N., Jan, L.Y. (1993). Primary structure and functional expression of a mouse inward rectifier potassium channel. *Nature* *362*, 127-133.

Kubo, Y., Reuveny, E., Slesinger, P. A., Jan, Y. N., and Jan, L. Y. (1993). Primary structure and functional expression of a rat G-protein-coupled muscarinic potassium channel. *Nature* *364*, 802-806.

Lesage, F., Attali, B., Lazdunski, M., and Barhanin, J. (1992). I_{SK} , a slowly activating voltage-sensitive K^+ channel characterization of multiple cDNAs and gene organization in the mouse. *FEBS* 301, 168-172.

Lopatin, A. N., Makina, E. N., and Nichols, C. G. (1994). Potassium channel block by cytoplasmic polyamines as the mechanism of intrinsic rectification. *Nature* 372, 366-369.

MacKinnon, R. (1991). Determination of the subunit stoichiometry of a voltage-activated potassium channel. *Nature* 350, 232-235.

Mason, D. E., Tomich, M. G., and Freeman, L. (1996). A minimal potassium channel underlies the slow K^+ current in pig ovarian granulosa cells. *Biophys. J.* 65, A:312.

Merot, J., Bidet, M., Le Maout, S., Tauc, M., and Poujeol, P. (1989). Two types of K^+ channels in the apical membrane of rabbit proximal tubule in primary culture. *Biochim. Biophys. Acta* 978, 134-144.

Miledi, R., and Parker, I. (1984). Chloride current induced by injection of calcium into *Xenopus* oocytes. *J. Phys.* 357, 173-183.

Mirroneau, J., and Savineau, J. (1980). Effects of calcium ions on outward membrane currents in rat uterine smooth muscle. *J. Phys.* 302, 411-425.

Moorman JR, P. C., John JE, Durieux ME, Jones LR (1992). Phospholemman expression induces a hyperpolarization-activated Chloride current in *Xenopus* oocytes. *J. Biol. Chem.* 267, 14551-14554.

Palmer, C. J., Scott, B. T., and Jones, L. R. (1991). Purification and complete sequence determination of the major plasma membrane substrate for cAMP-dependent proteinKinase and proteinKinase C in myocardium. *J. Biol. Chem.* 266, 11126-11130.

Parker, I., Miledi, R. (1988). A calcium-dependent chloride current activated by hyperpolarization in *Xenopus* oocytes. *Proc. R. Soc. Lond.* 233, 191-199.

Pinto LH, H. L., Lamb RA (1992). Influenza virus M₂ protein has ion channel activity. *Cell* 69, 517-528.

Pongs, C., Kecskemethy, N., Muller, R., Krah-Jentgens, I., Baumann, A., Kiltz, H. H., Canal, I., Llamazares, S., and Ferrus, A. (1988). *Shaker* encodes a family of putative potassium channel proteins in the nervous system of drosophila. *EMBO J* 7, 1087-1096.

Pragnell, M., Snay, K. J., Trimmer, J. S., MacLusky, N. J., Naftolin, F., Kaczmarek, L. K., and Boyle, M. B. (1990). Estrogen induction of a small, putative K⁺ channel mRNA in rat uterus. *Neuron* 4, 807-812.

Salkoff, L., Baker, K., Butler, A., Corvarrubias, M., and Pak, M. (1992). An essential 'set' of K⁺ channels conserved in flies, mice, and humans. *TINS* 15, 161-166.

Sanguinetti, M. C., and Jurkiewicz, N. K. (1991). Delayed rectifier outward K^+ current is composed of two currents in guinea pig atrial cells. *Am. Phys. Soc.* 393-399.

Sanguinetti, M. C., and Jurkiewicz, N. K. (1990). Two components of cardiac delayed rectifier K^+ current. *J. Gen. Phys.* 96, 195-215.

Stefani, E., Toro, L., Perozo, E., and Bezanilla, F. (1994). Gating of Shaker K^+ : I. Ionic and gating currents. *Biophys. J.* 66, 996-1010.

Sugimoto, T., Tanabe, Y., Shigemoto, R., Iwai, M., Takumi, T., Ohkubo, H., and Nakanishi, S. (1990). Immunohistochemical study of a rat membrane protein which induces a selective potassium permeation: its localization in the apical membrane portion of epithelial cells. *J. Mem. Bio.* 113, 39-47.

Swanson, R., Marshall, J., Smith, J. S., Williams, J. B., Boyle, M. B., Folander, K., Luneau, C. J., Antanavage, J., Oliva, C., Buhrow, S. A., Bennett, C., Stein, R. B., and Kaczmarek, L. K. (1990). Cloning and expression of cDNA and genomic clones encoding three delayed rectifier potassium channels in rat brain. *Neuron* 4, 929-939.

Tagliatela, M., Kirsch, G. E., VanDongen, A. M. J., Drewe, J. A., Hartmann, H. A., Joho, R. H., Stefani, E., and Brown, A. M. (1992). Gating currents from a delayed rectifier K^+ channel with altered pore structure and function. *Biophys. J.* 62, 34-36.

Takumi, T., Moriyoshi, K., Aramori, I., Ishii, T., Oiki, S., Okada, Y., Ohkubo, H., and Nakanishi, S. (1991). Alteration of channel activities and gating by mutations of slow I_{SK} potassium channels. *J. Biol. Chem.* 266, 22192-22198.

Takumi, T., Ohkubo, H., and Nakanishi, S. (1988). Cloning of a membrane protein that induces a slow voltage-gated potassium current. *Science* 242, 1042-1045.

Tempel, B. L., Papazian, D. M., Schwarz, T. L., Jan, Y. N., and Jan, L. Y. (1987). Sequence of a probable potassium channel component encoded at *Shaker* locus of *Drosophila*. *Science* 237, 770-775.

Timpe, L. C., Jan, Y. N., and Jan, L. Y. (1988). Four cDNA clones from the *Shaker* locus of *Drosophila* induce kinetically distinct A-type potassium currents in *Xenopus* oocytes. *Neuron* 1, 659-667.

Timpe, L. C., Schwarz, T. L., Tempel, B. L., Papazian, D. M., Jan, Y. N., and Jan, L. Y. (1988). Expression of functional potassium channels from *Shaker* cDNA in *Xenopus* oocytes. *Nature* 331, 143-145.

Tzounopoulos, T., Adelman, J. P., and Maylie, J. (1996). Gating mechanism of minK channels expressed in *Xenopus* oocytes (in press).

Tzounopoulos, T., Guy, H. R., Durrel, S., Adelman, J. P., and Maylie, J. (1995). minK channels form by assembly of at least 14 subunits. *Proc. Nat. Acad. Sci. USA*, 9593-9597.

- Tzounopoulos, T., Maylie, J., and Adelman, J. P. (1995). Induction of endogenous channels by high levels of heterologous membrane proteins in *Xenopus* oocytes. *Biophys. J.* *79*, 904-908.
- Varnum, M. D., Busch, A. E., Bond, C. R., Maylie, J., and Adelman, J. P. (1994). The minK channel underlies the cardiac potassium current I_{Ks} and mediates species-specific responses to proteinKinase C. *Proc. Natl. Acad. Sci. USA* *90*, 11528-11532.
- Wang, K. W., Tai, K. K., and Goldstein, S. A. N. (1996). MinK residues line a potassium channel pore. *Neuron* *19*, 1650-1655.
- Wang, K. W., Tai, K. K., and Goldstein, S. A. N. (1995). Subunit composition of minK channels. *Neuron* *14*, 1303-1309.
- Wettwer, E., Scholtysik, G., Schaad, A., Himmel, H., and Ravens, U. (1991). Effects of the new class III antiarrhythmic drug E-4031 on myocardial contractility and electrophysiological parameters. *J. Cardio. Pharm.* *17*, 480-487.
- Yamane, T., Furukawa, T., Horikawa, S., and Hiraoka, M. (1993). External pH regulates the slowly activating potassium current I_{sK} expressed in *Xenopus* oocytes. *FEBS* *319*, 229-232.
- Yang, J., Jan, Y. N., and Jan, L. Y. (1995). Determination of the subunit stoichiometry of an inwardly rectifying potassium channel. *Neuron* *15*, 1441-1447.
- Yang, Y., and Sigworth, F. (1995). The conductance of minK channels is very small. *Biophys. J.* *68*, A:22.

Zagotta, W. N., Hoshi, T., Dittman, J., Aldrich, R.W. (1994). Shaker potassium channel gating II: Transitions in the activation pathway. *J. Gen. Phys.* *103*, 279-313.